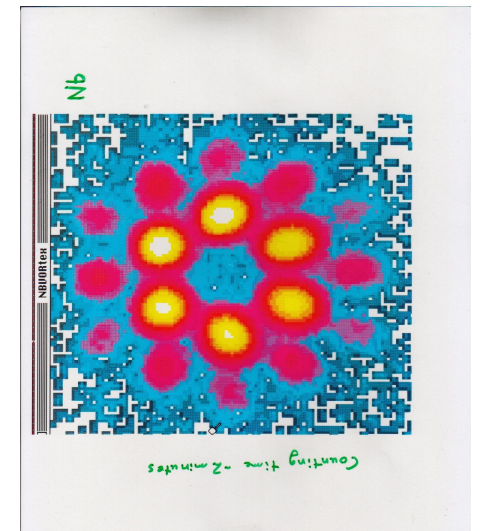
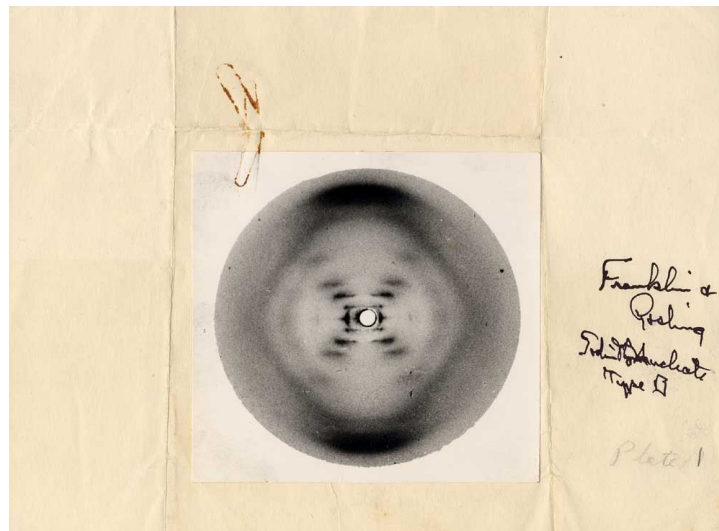
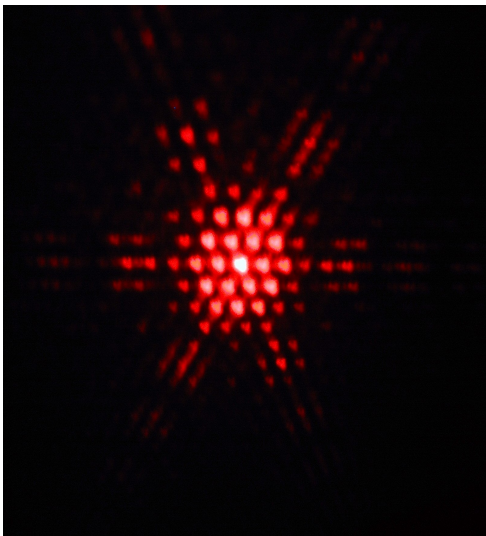


Scattering, Diffraction, Material Particles and Waves

C.F.Majkrzak
NIST Center for Neutron Research

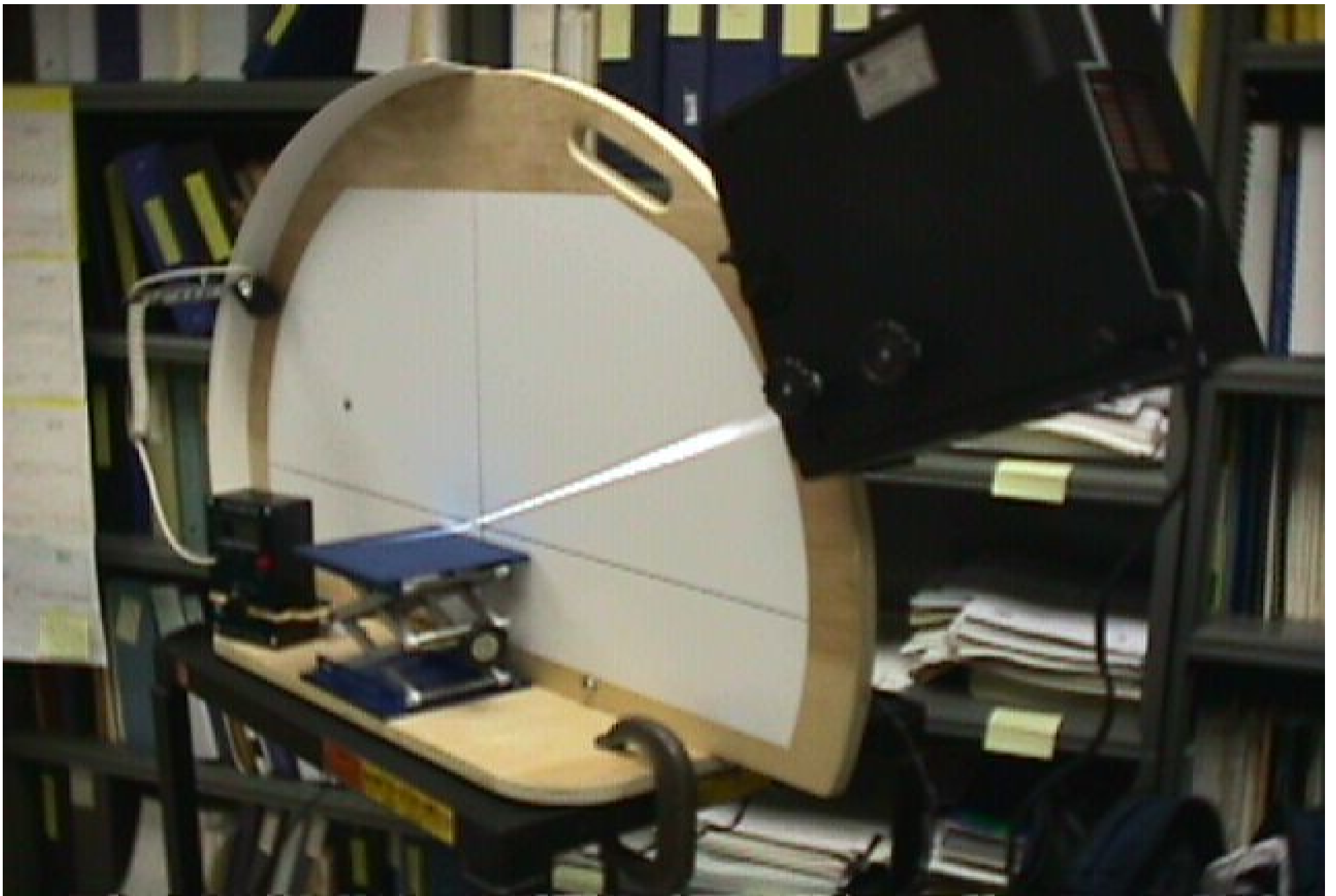
Neutron Scattering School, June 2012



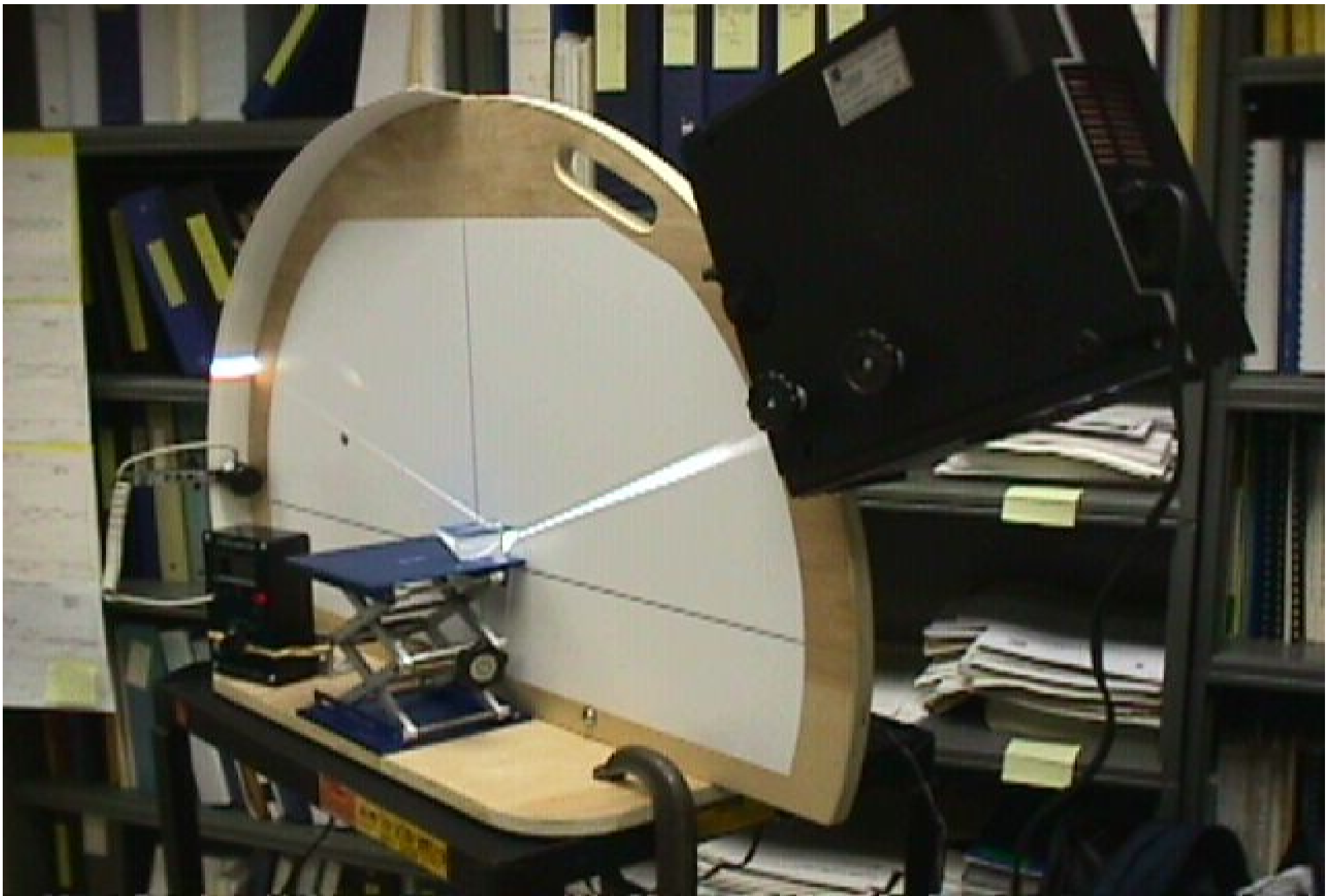
(Hexagonal aperture optical diffr. pattern – J.Newman, Union.edu) (DNA x-ray diffraction pattern - R.Franklin) (superconducting Nb vortex lattice neutron diffraction pattern – J.Lynn et al.)



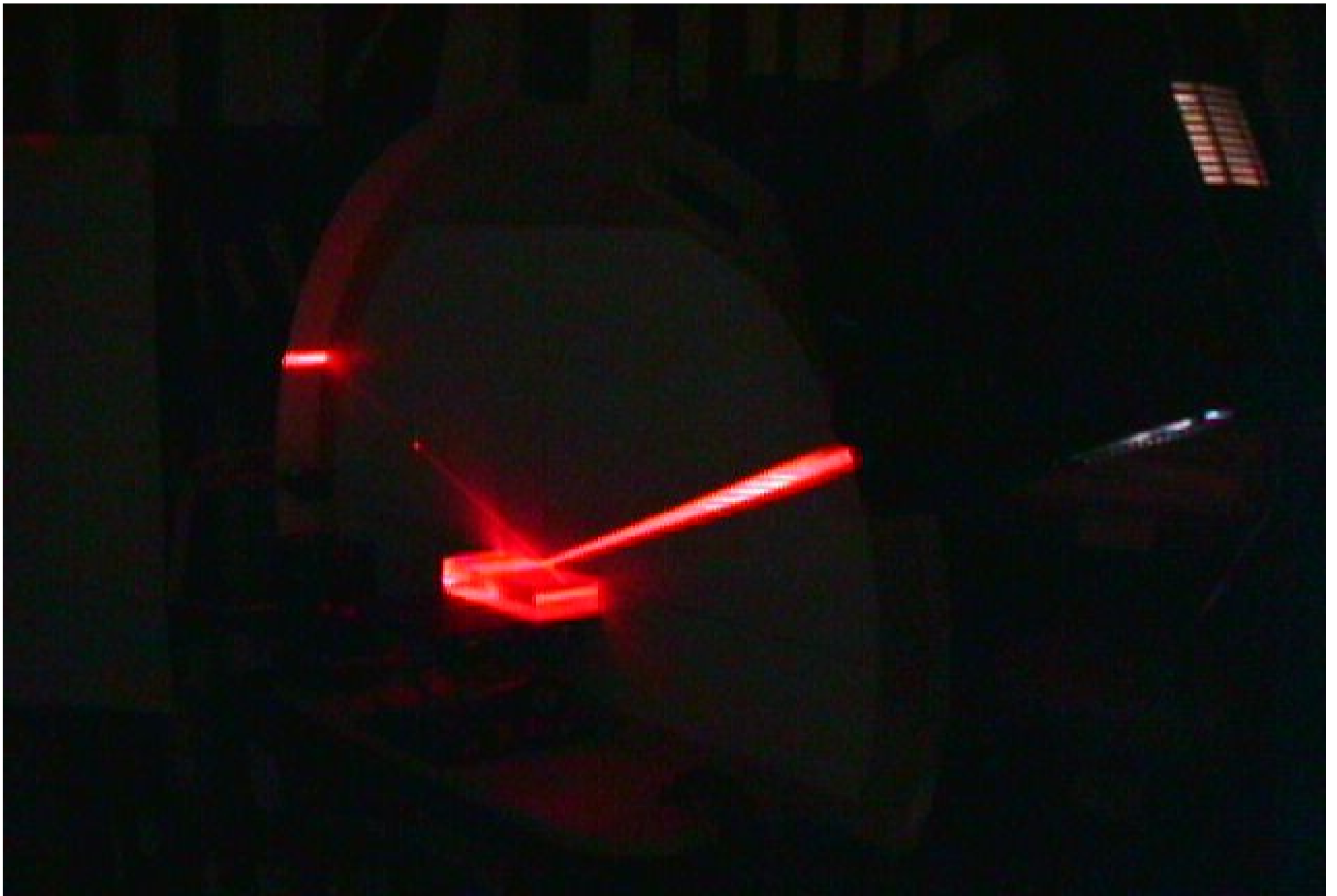
Angularly divergent white light source.



Angularly collimated white beam.

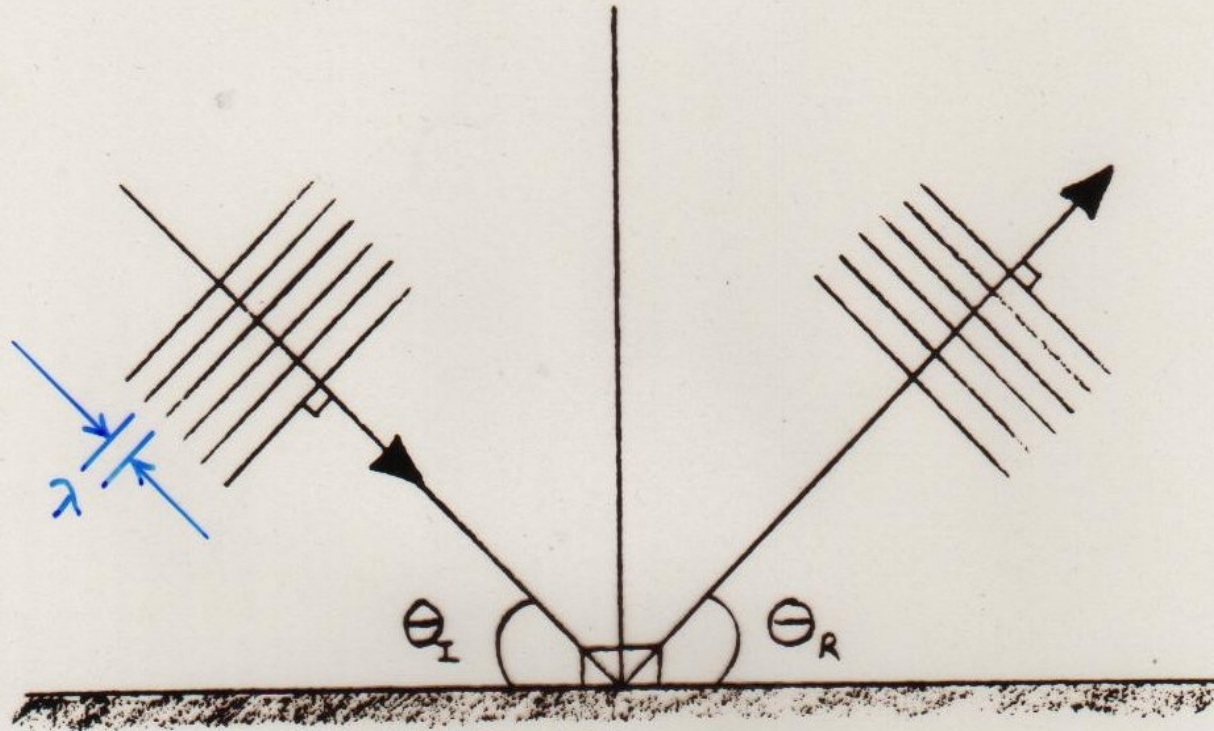


Collimated white beam specularly reflected.



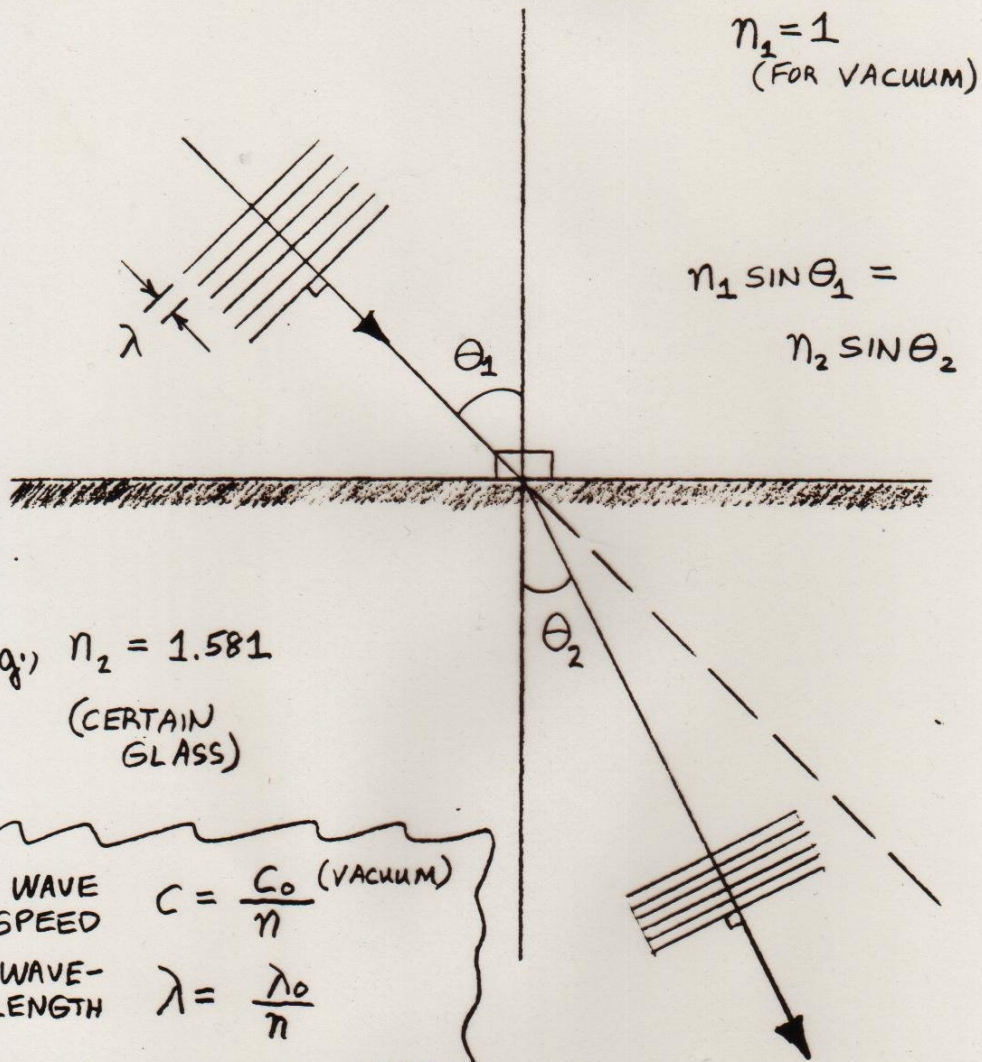
Monochromatic, collimated beam specularly reflected.

"SPECULAR" OR "MIRROR" REFLECTION
OF A WAVE



ANGLE OF INCIDENCE θ_I
= ANGLE OF REFLECTION θ_R

REFRACTION OF A LIGHT WAVE



WAVE SPEED $c = \frac{c_0 \text{ (VACUUM)}}{n}$

WAVE-LENGTH $\lambda = \frac{\lambda_0}{n}$

WAVE-VECTOR $k = nk_0 = \frac{2\pi\nu}{c}$

FREQUENCY $\nu = \text{CONSTANT}$

REFRACTIVE INDEX n DEPENDS ON MATERIAL AND WAVELENGTH OF THE LIGHT

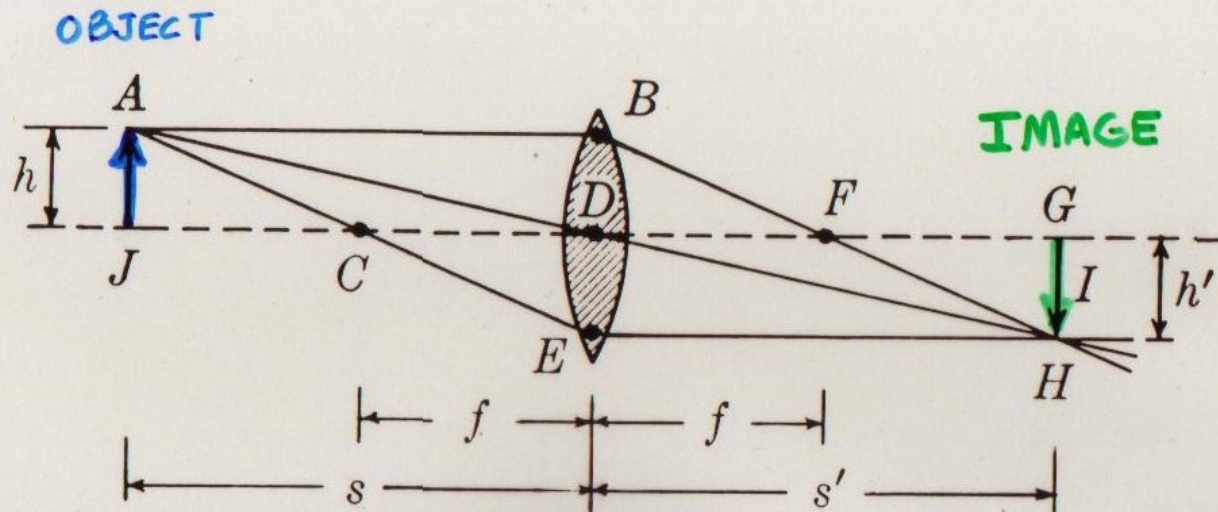


Figure 44-10. Geometrical relations among object distance s , image distance s' , and focal length f .

(from Weidner & Sells, *Elementary Classical Physics*)

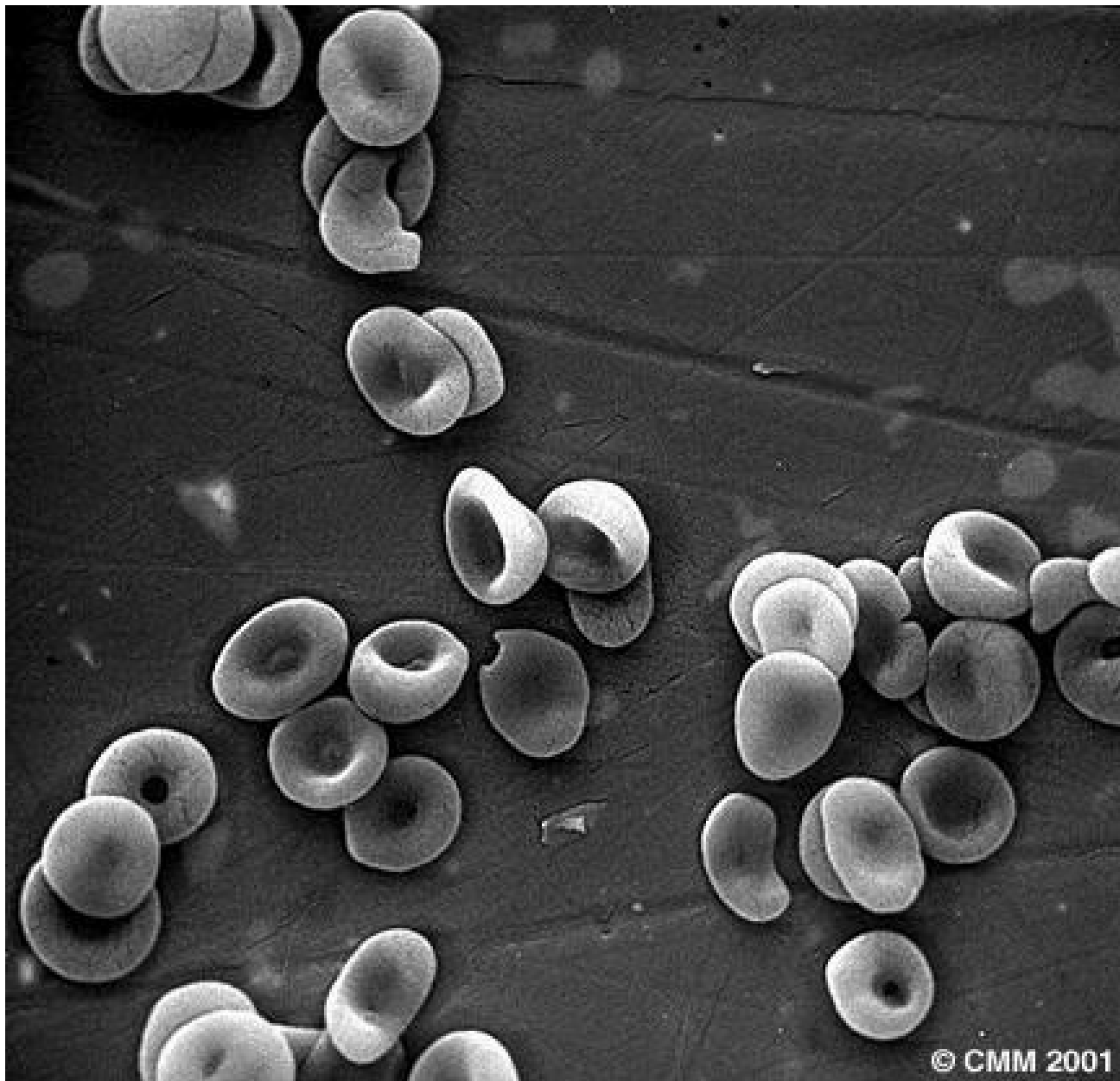
$$\frac{1}{f} = \frac{1}{s} + \frac{1}{s'}$$

$$\frac{h}{s} = \frac{h'}{s'}$$

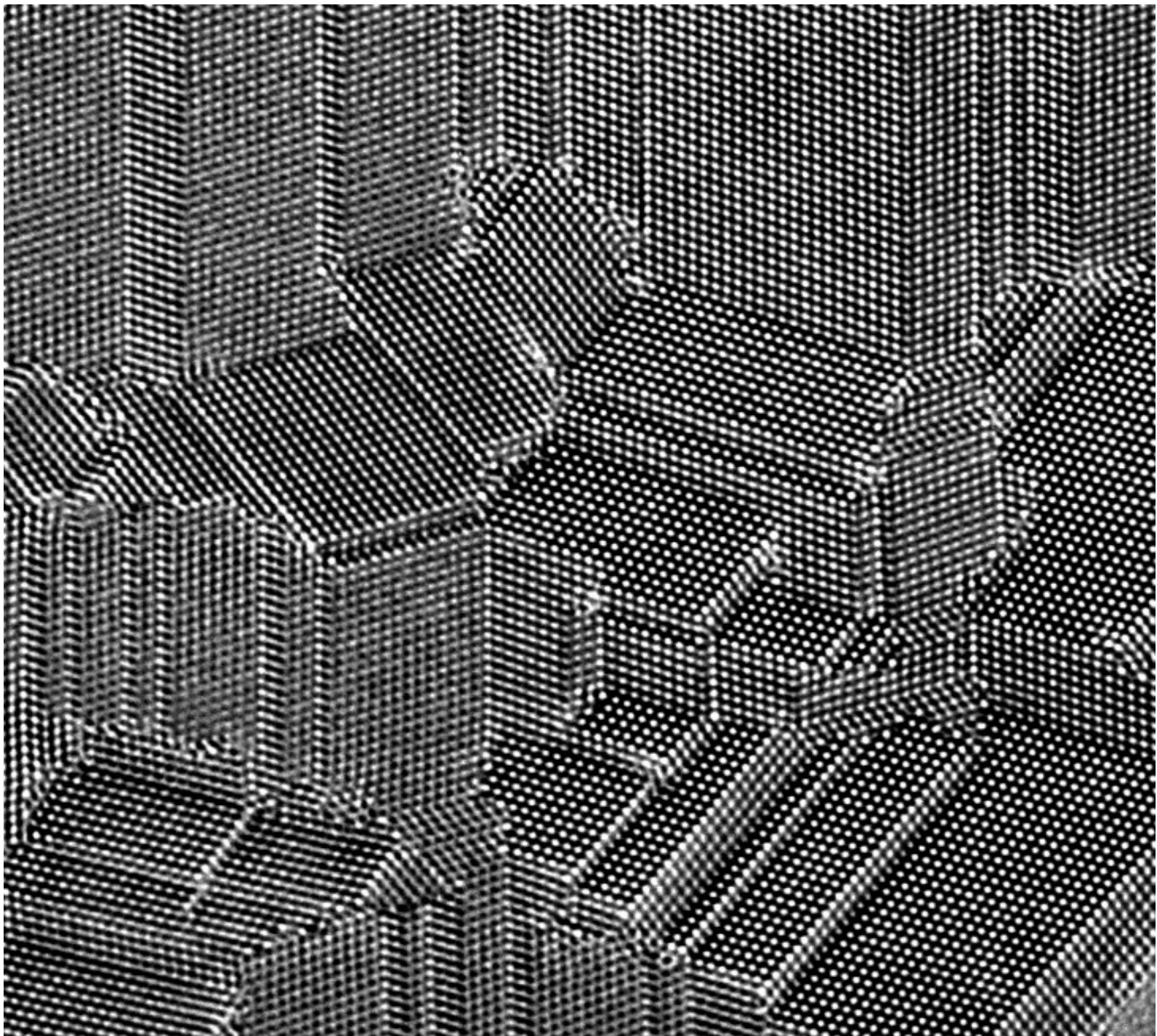
The ratio of image-object *distances*, s'/s , is equal to the ratio of in-
object *sizes*, h'/h . This ratio h'/h is known as the *lateral magnification*.



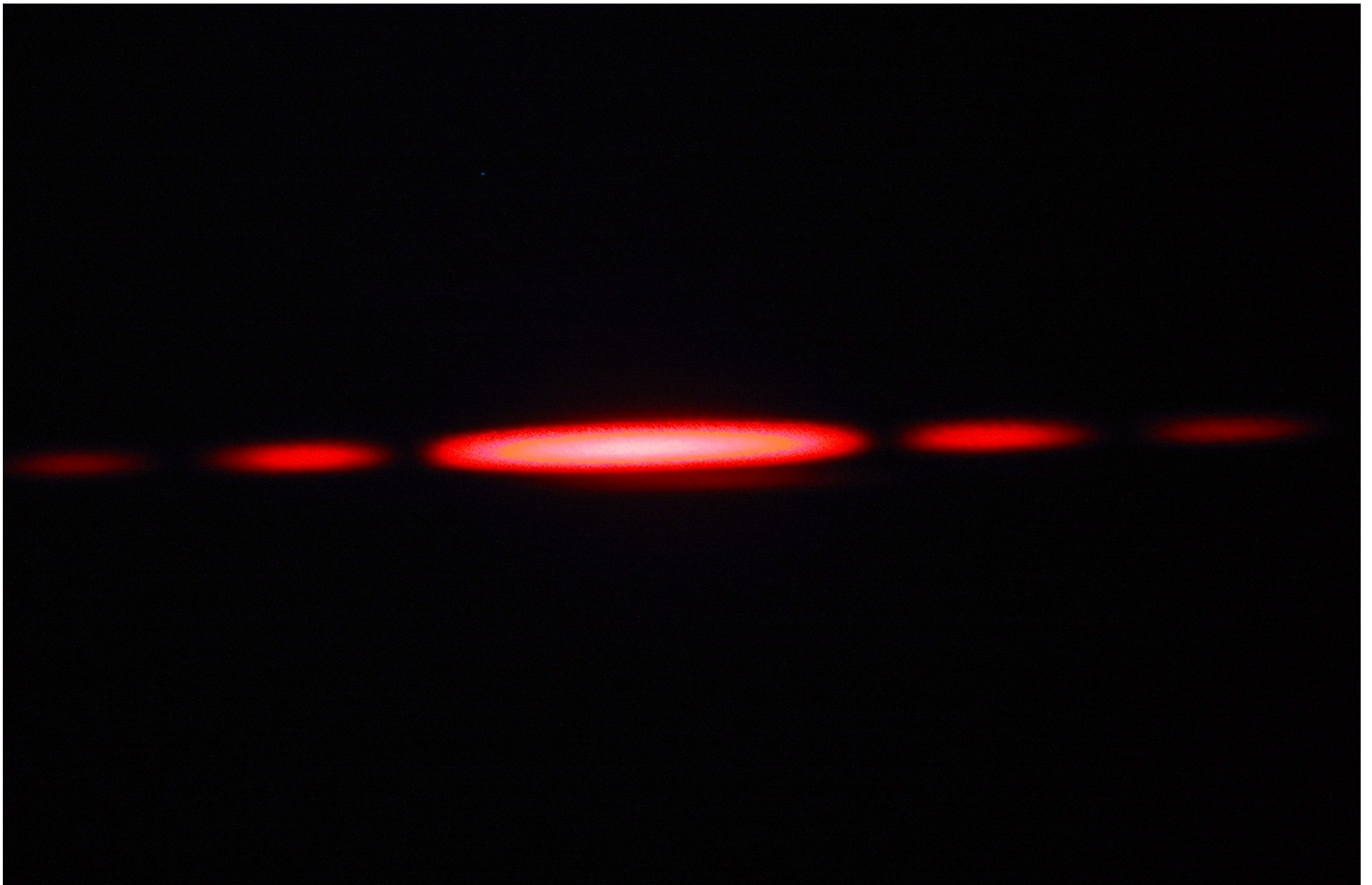
Flea head, 170 x magnification, scanning electron microscope, www.uq.edu.au (University of Queensland, Australia, Center for Microscopy and Microanalysis).



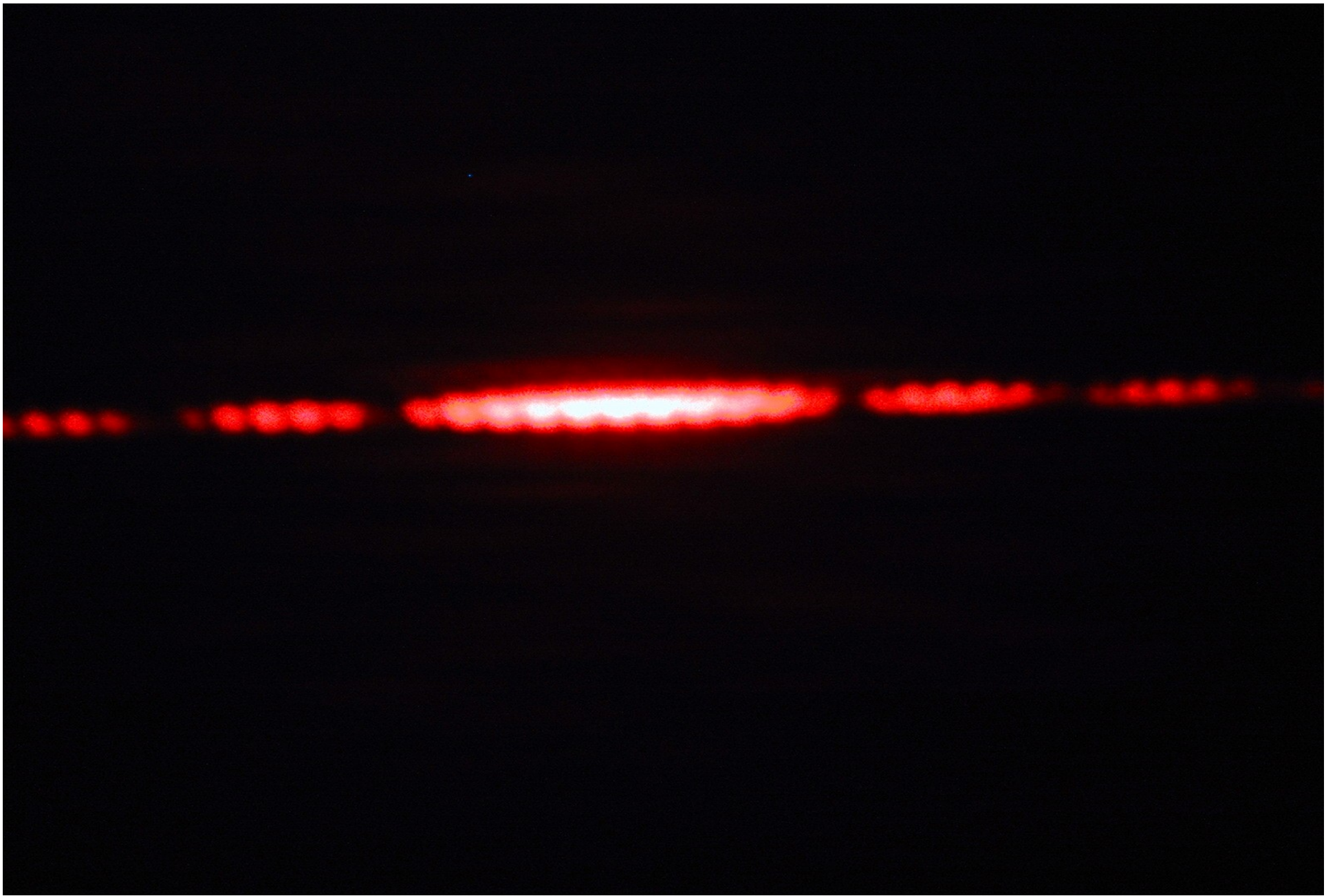
Blood cells, 2000 x magnification, scanning electron microscope, www.uq.edu.au.



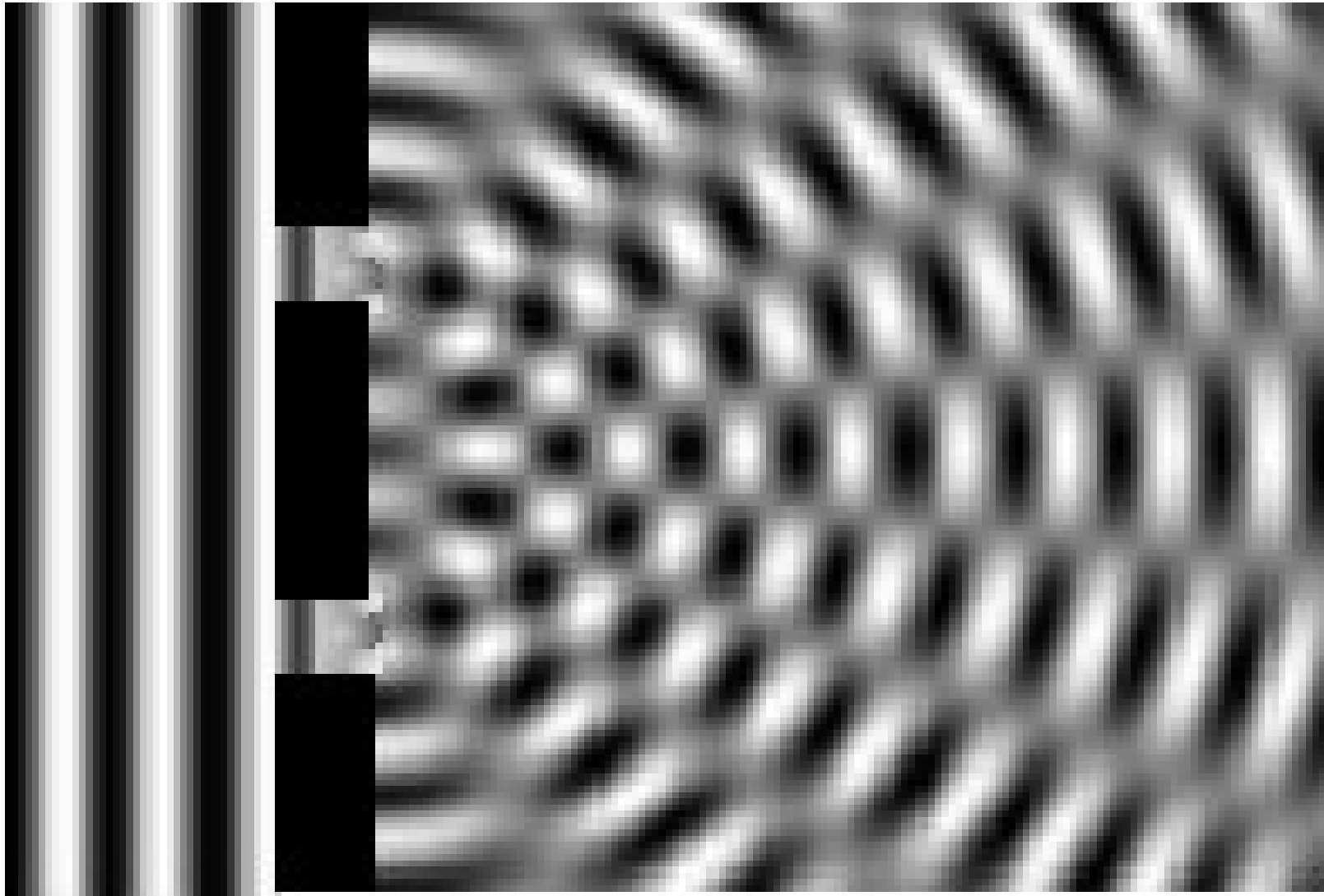
Atomic resolution micrograph of multiply-twinned nanocrystalline film of Si. (C. Song)



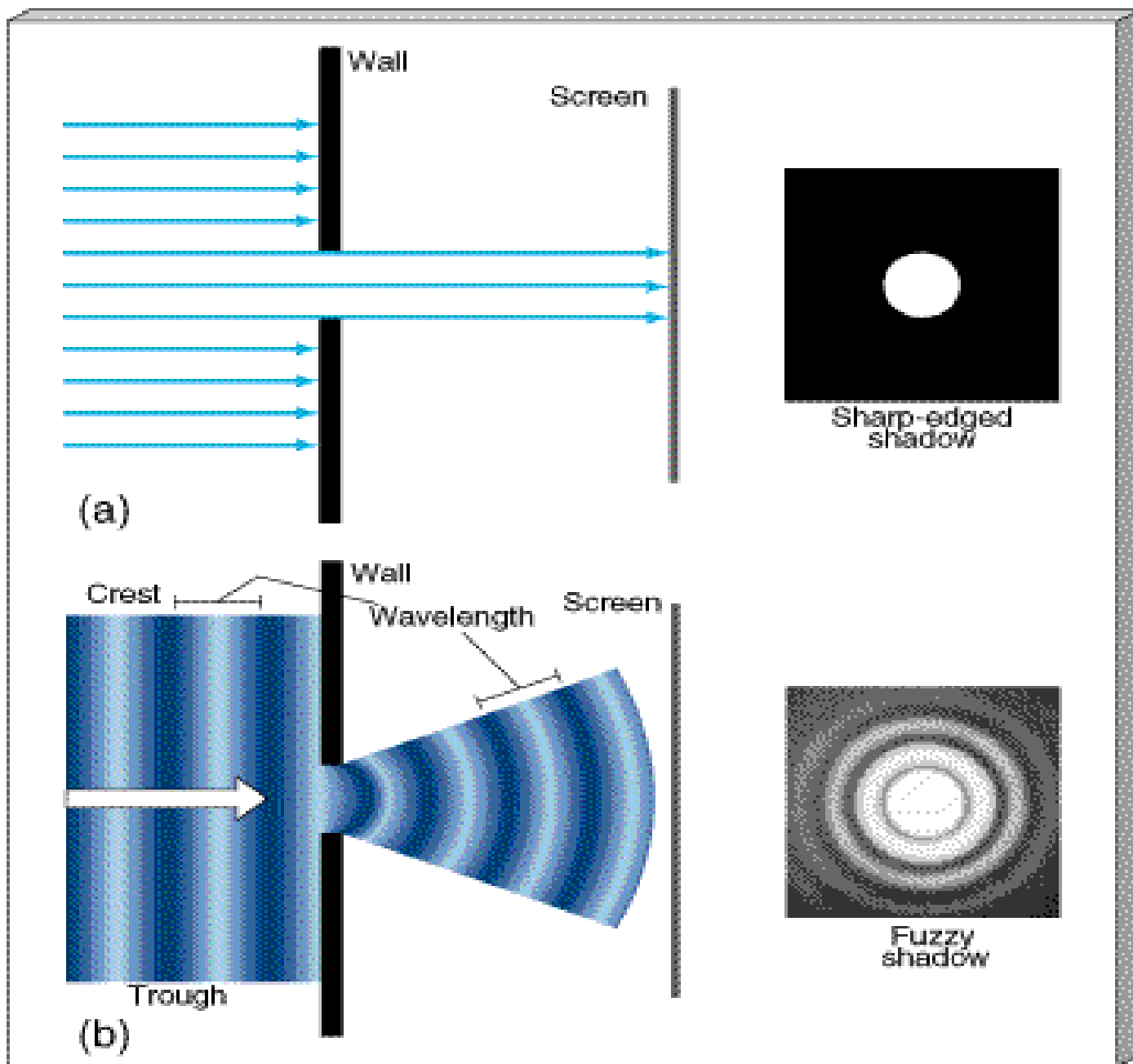
Single slit monochromatic light diffraction – Maleki/Newman at www1.union.edu.



Double slit monochromatic light diffraction – Maleki/Newman at www1.union.edu.



Water wave diffracting through a double aperture (from left to right) – B.Crowell,
Light and Matter, www.vias.org/physics.



(from Photonics
by Saleh & Teich)

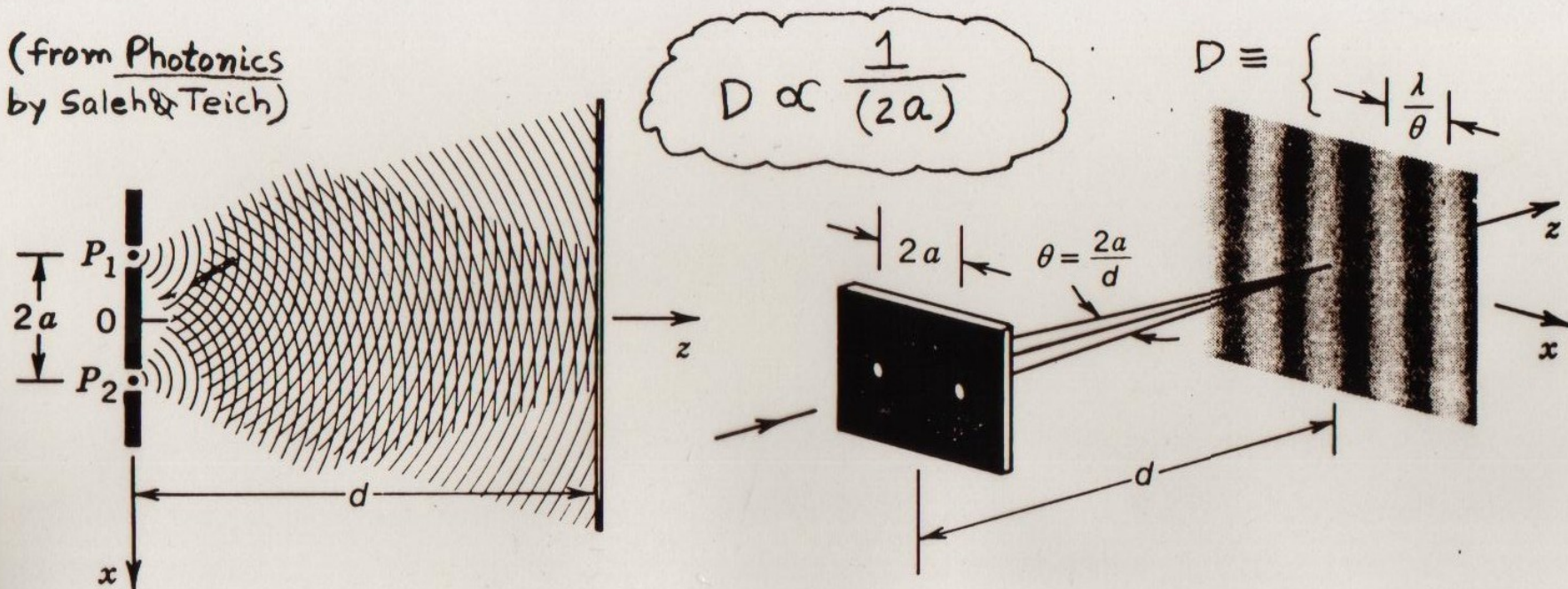
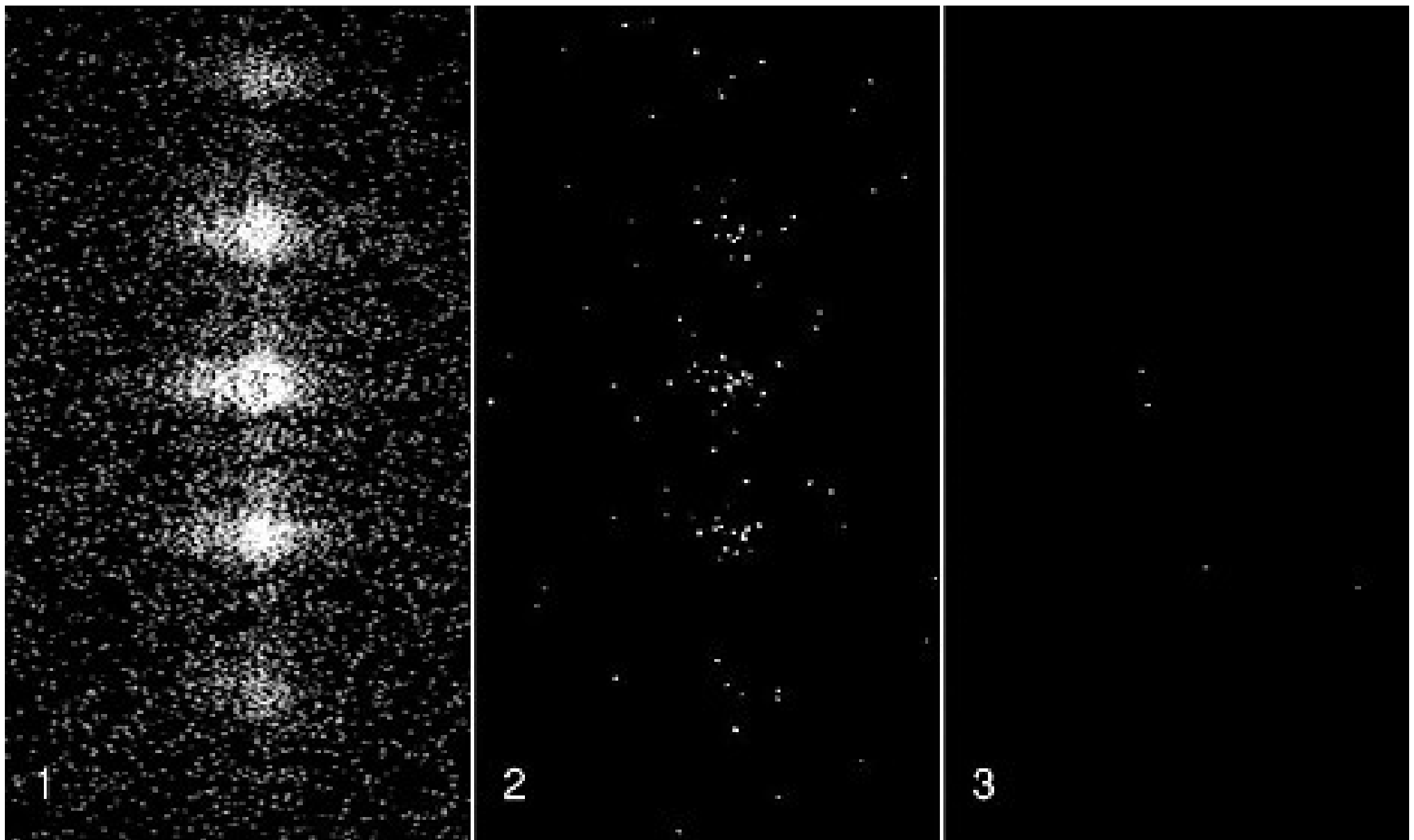


Figure 2.5-6 Interference of two spherical waves of equal intensities originating at the points P_1 and P_2 . The two waves can be obtained by permitting a plane wave to impinge on two pinholes in a screen. The light intensity at an observation plane a distance d away takes the form of a sinusoidal pattern with period $\approx \lambda/\theta$.

DIFFRACTION PATTERN WHICH RESULTS FROM THE COHERENT SUPERPOSITION OF TWO WAVES (AMPLITUDES OF THE TWO WAVES ADD TOGETHER AT ANY GIVEN POINT IN SPACE)

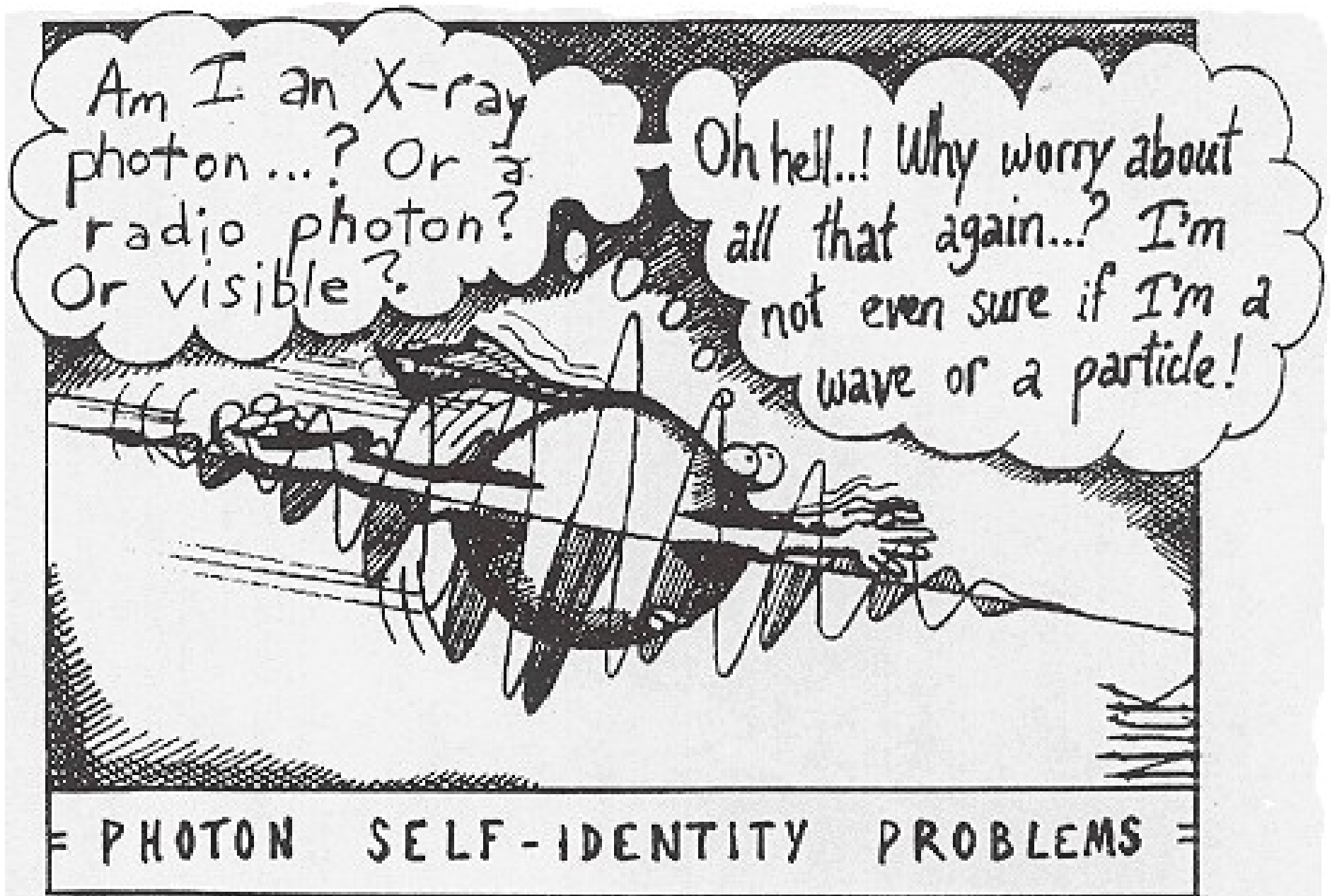
A CHARACTERISTIC RECIPROCAL RELATIONSHIP EXISTS BETWEEN THE POSITIONS OF THE INTENSITY MAXIMA IN THE DIFFRACTION PATTERN AND THE DISTANCE SEPARATING THE OBJECTS CAUSING THE SCATTERING.



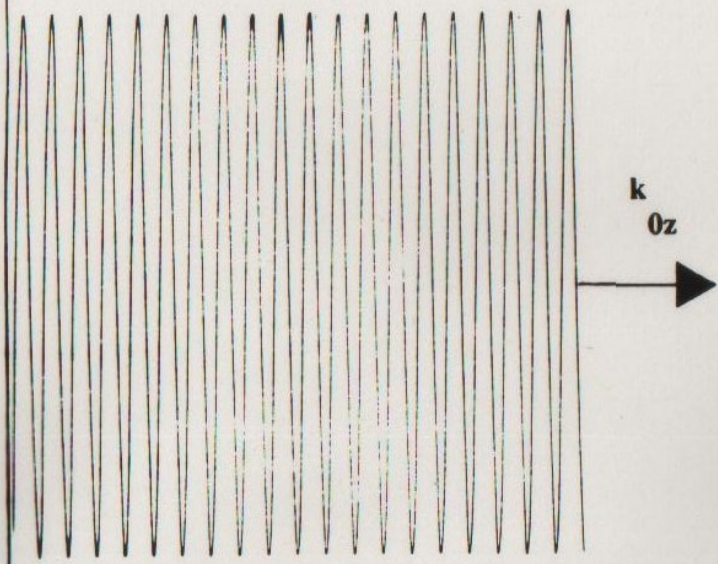
Wave interference patterns produced by monochromatic laser light diffracting through a triple slit aperture for various intensities – L.Page (www.vias.org/physics). This is a dramatic illustration of wave-particle duality.



X-ray transmission image.



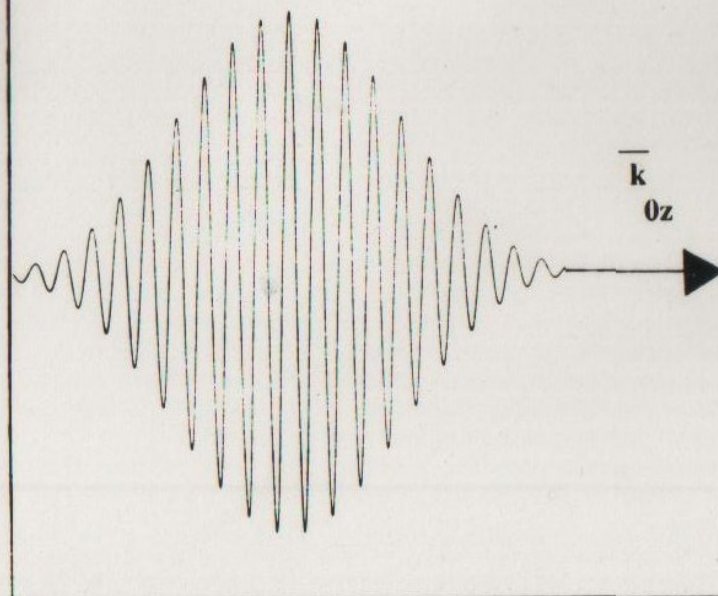
Plane Wave Amplitude



a)

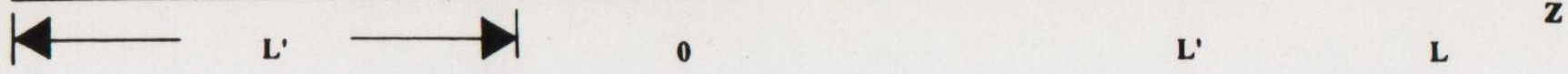
SLD

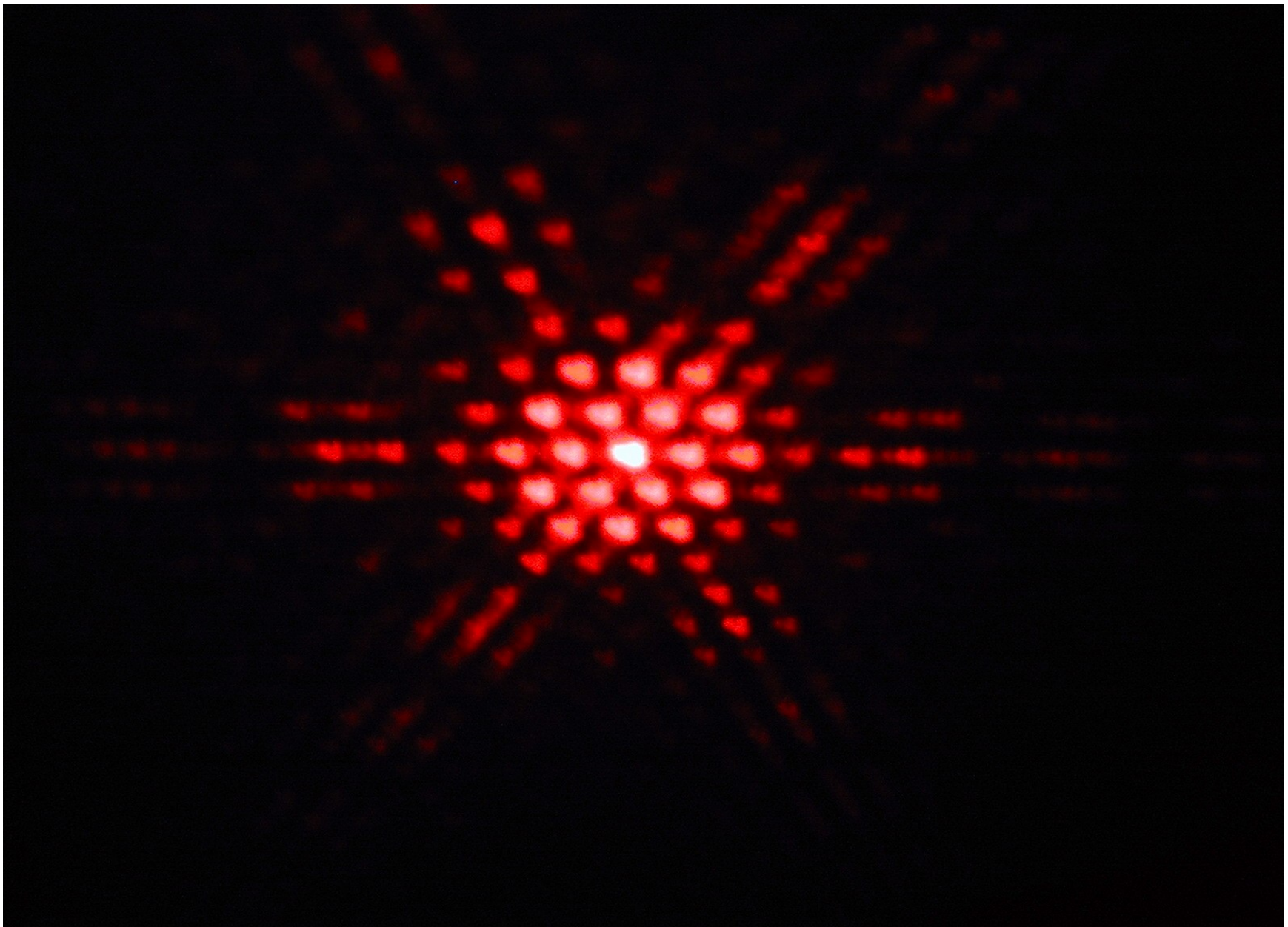
Wave Packet Amplitude



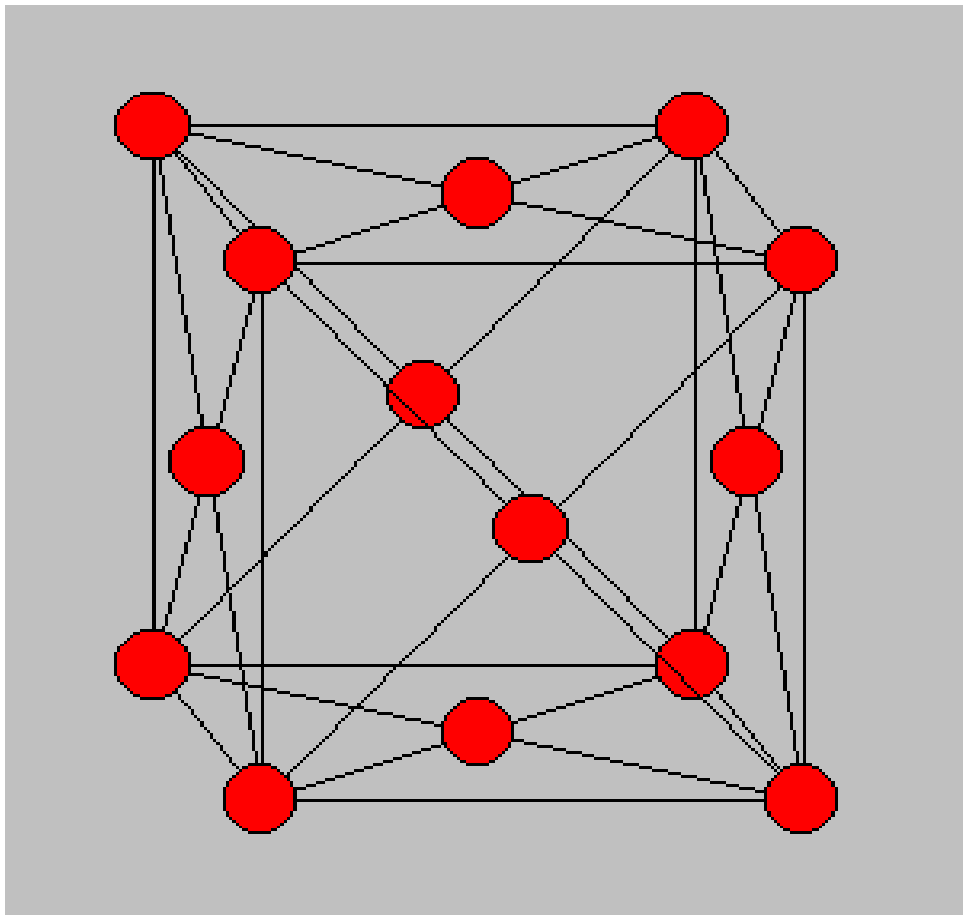
b)

SLD





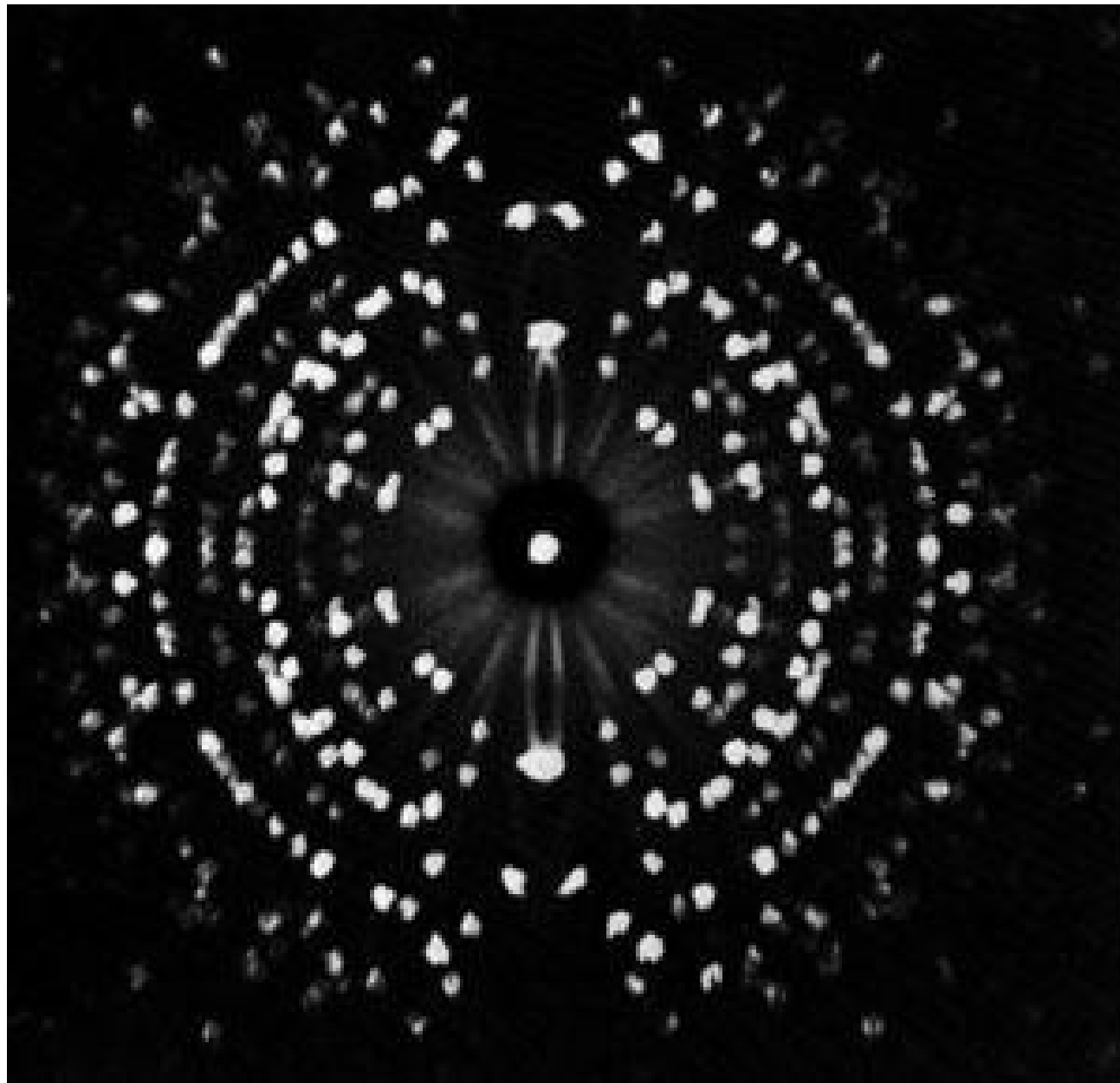
Hexagonal aperture monochromatic light diffraction – Maleki/Newman at www1.union.edu.



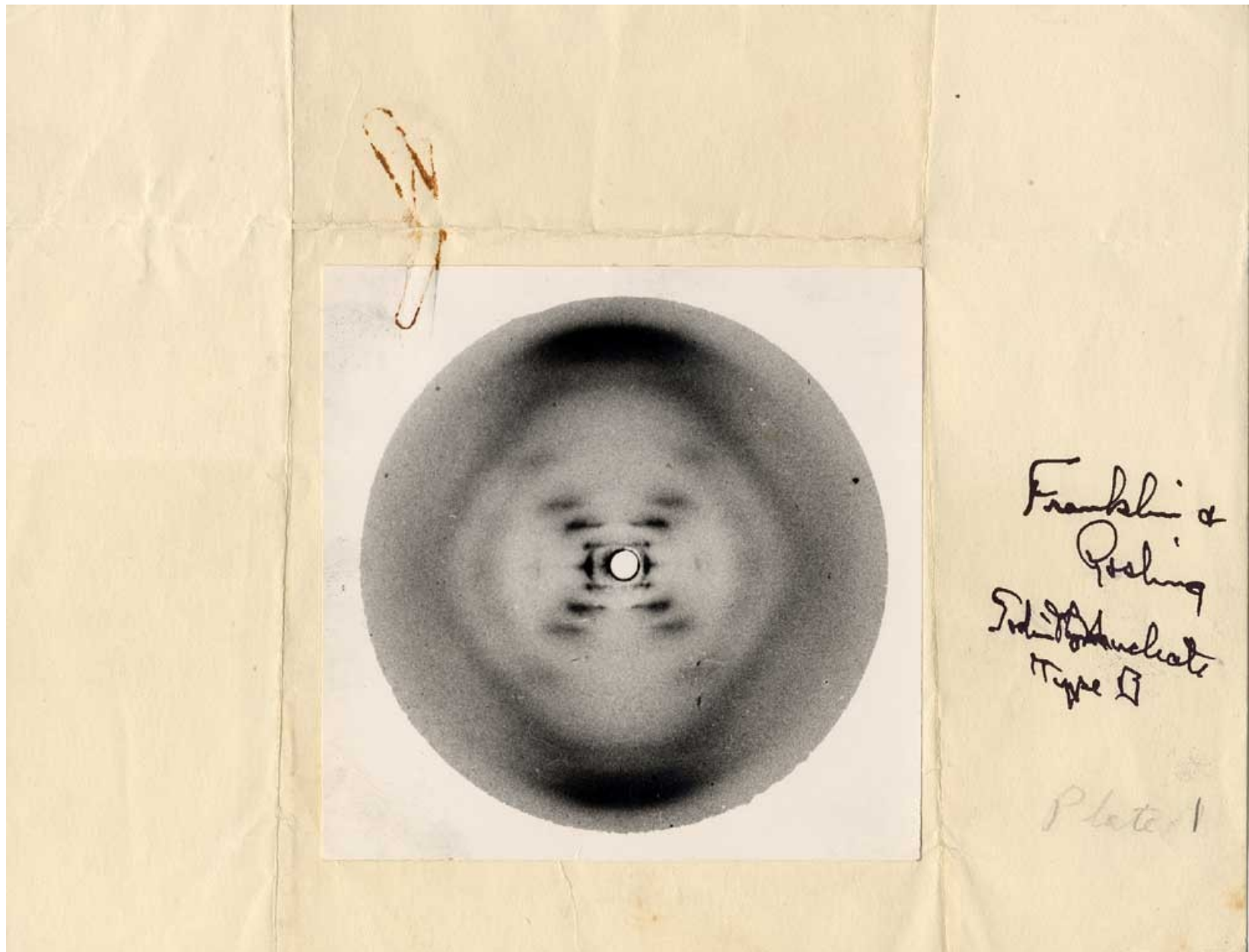
FCC aluminum crystal structure -
colorado.edu.



Electron diffraction pattern for aluminum -
canemco.com.



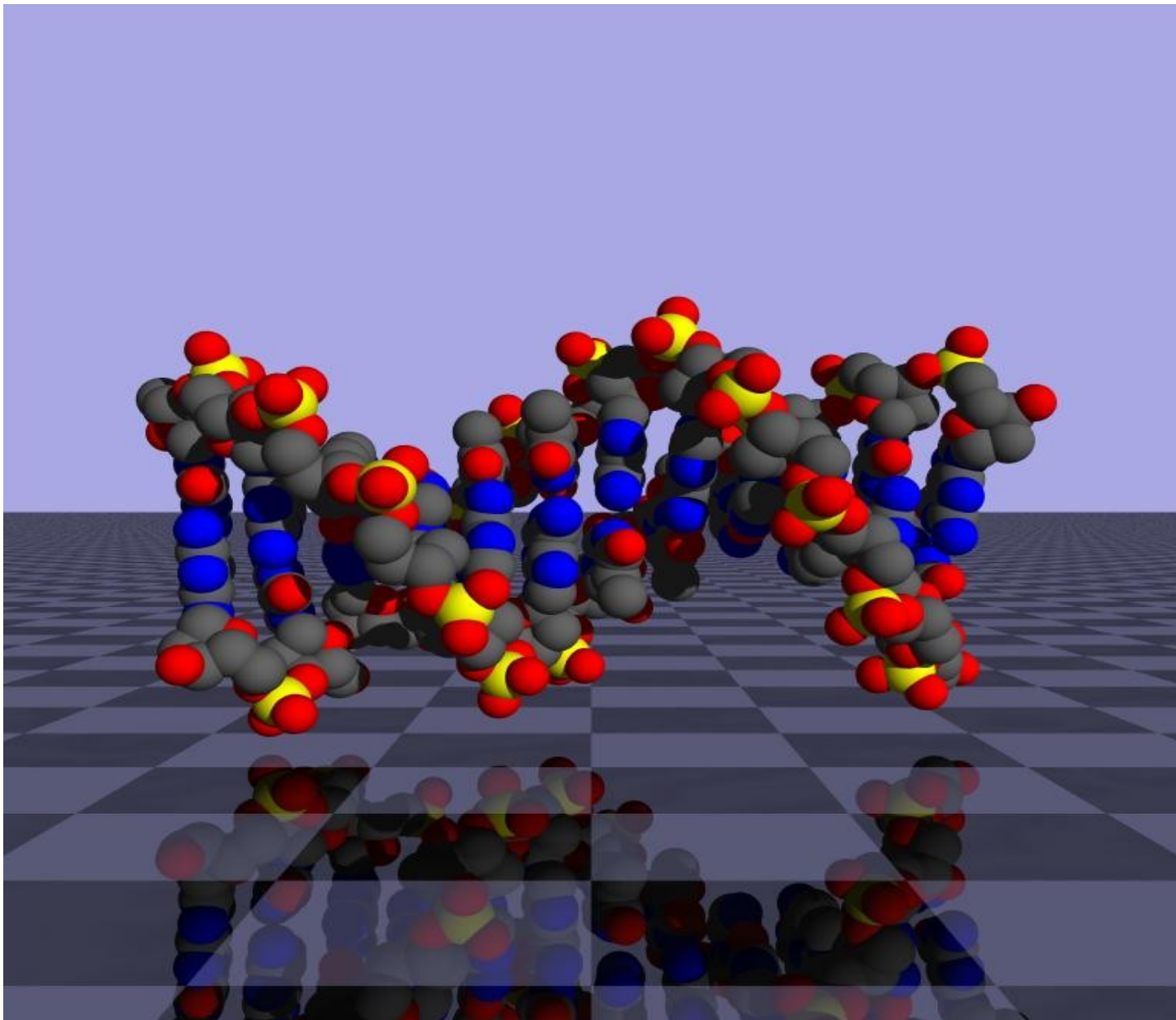
Electron diffraction pattern for a single alum crystal – H.J.Milledge, Department of Geology, University College, London.



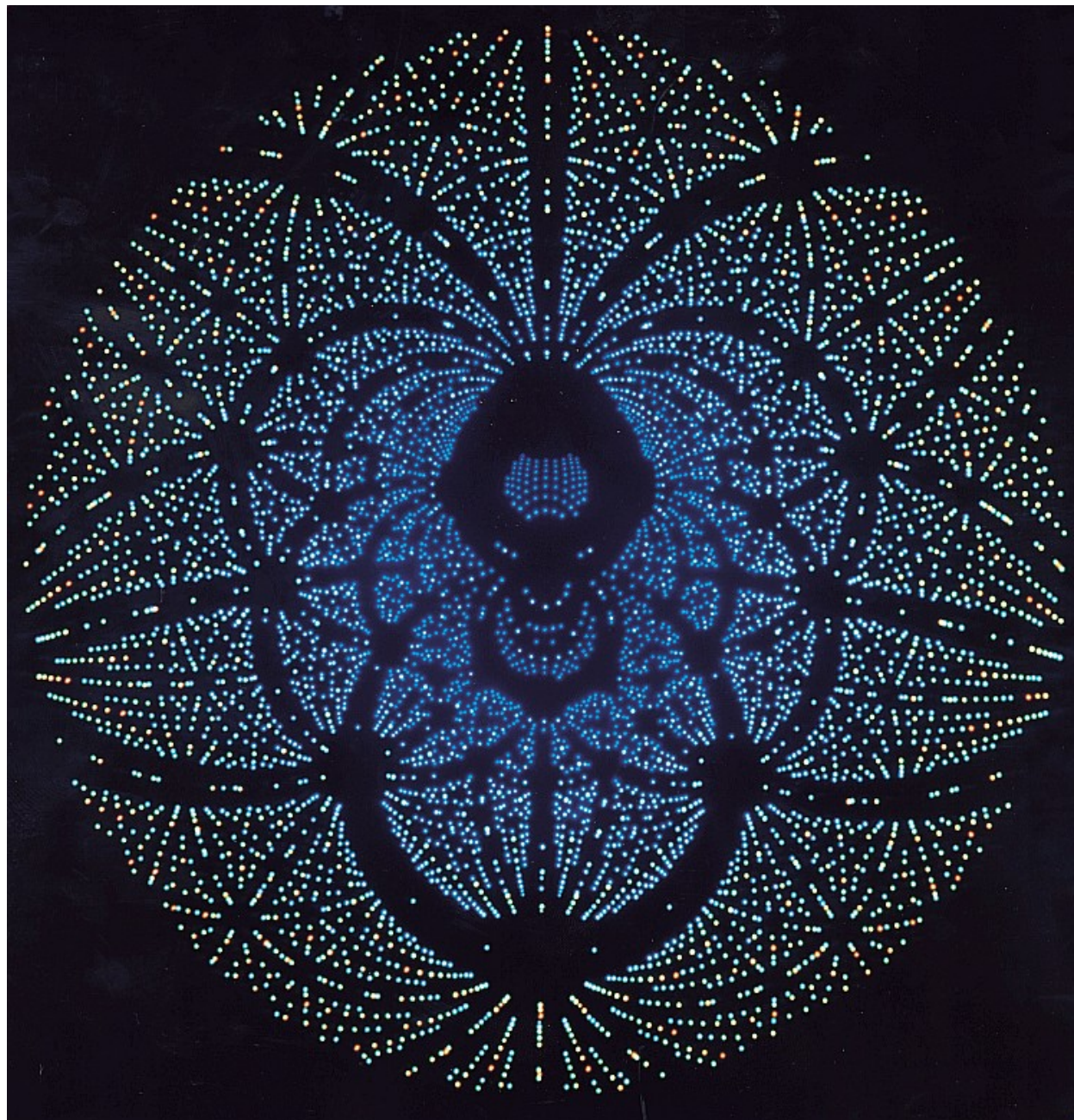
Franklin &
Gosling
DNA structure
Type I

Plate 1

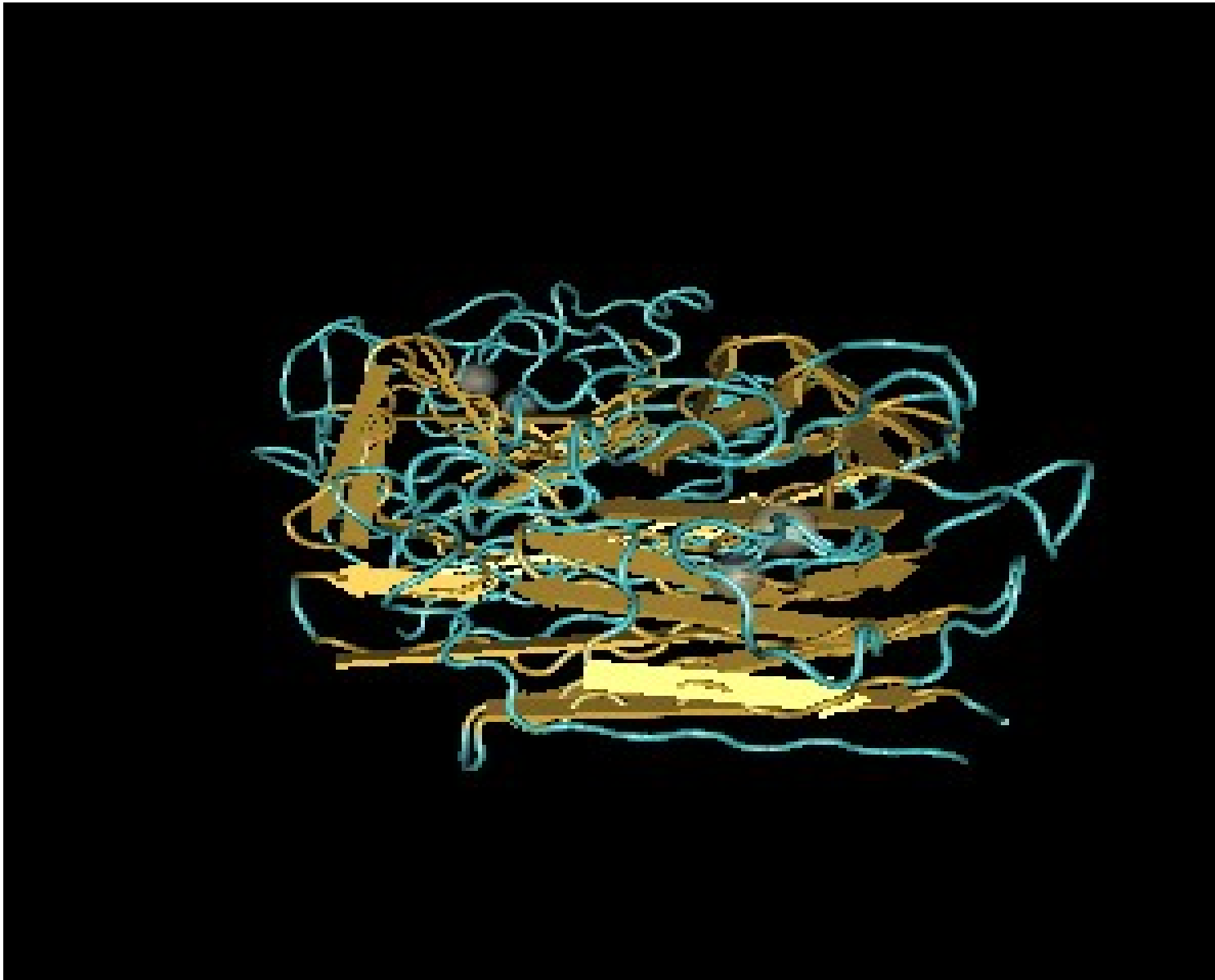
X-ray diffraction pattern for DNA obtained by Rosalind Franklin.



Model of DNA structure – academy.d20.co.edu.



X-ray diffraction pattern from a protein, lectin, found in peas – CCLRC Synchrotron Radiation Source, Daresbury Laboratory, UK.



Reconstruction of atomic groups in the molecular structure of lectin, an important sugar-binding protein that plays a role in biological recognition phenomena within a living cell, based on x-ray diffraction measurements (prasthofer_pea_lectin_mmdimage.fcgi.png).

PROBES OF THE MICROSTRUCTURE OF SURFACES AND INTERFACES

photons, electrons, neutrons, atom and ion beams, miniature mechanical devices

* DIRECT IMAGING (REAL SPACE)

e.g.:

- optical microscopy (~ 1000 x magnification)
- scanning electron microscopy (SEM) (orders of magnitude higher magnification than possible with light)
- transmission electron microscopy (TEM)
- atomic force microscopy (AFM)

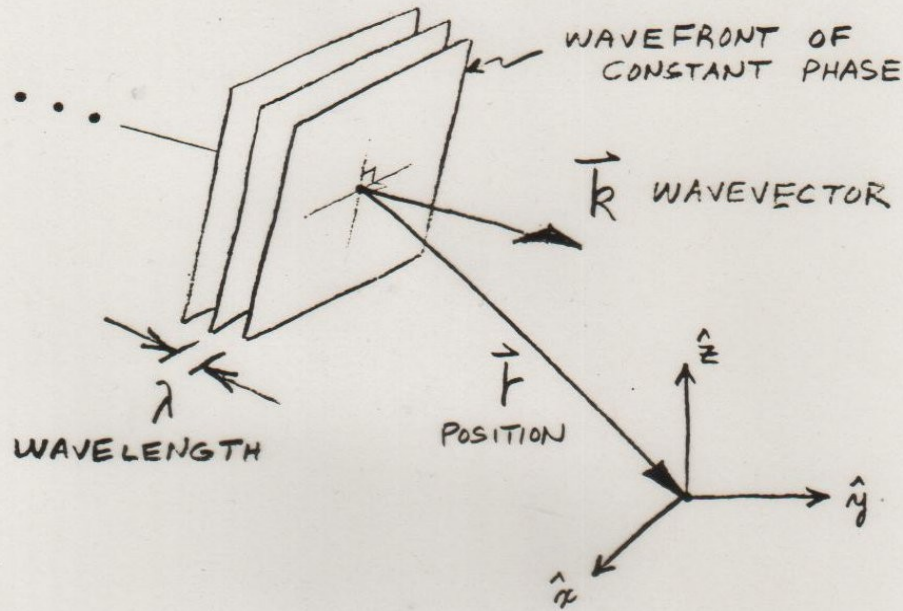
* DIFFRACTION (RECIPROCAL SPACE)

e.g.:

- low energy electron diffraction (LEED)
- spin polarized LEED (SPLEED)
- reflection high energy electron diffraction (RHEED)
- ellipsometry (optical polarimetry)
- x-ray reflectometry
- neutron reflectometry

For quantitative measurements of depth profiles along a normal to the surface, x-ray and neutron reflectometry are particularly useful because of their relatively weak interactions with condensed matter and the fact that these interactions can be described accurately by a comparatively simple theory. In the case of electron diffraction, on the other hand, the potential is non-local and the scattering is non-spherical, relatively strong and highly energy-dependent. For atom diffraction, the description of the interaction potential can be even more complicated.

THE NEUTRON AS A PLANE WAVE PROPAGATING IN FREE SPACE



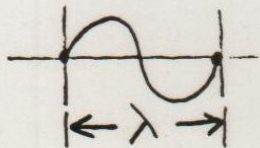
WAVEFUNCTION

$$\Psi \propto e^{i \vec{k}_0 \cdot \vec{r}}$$

$$\begin{cases} \vec{k}_0 = k_{0x} \hat{x} + k_{0y} \hat{y} + k_{0z} \hat{z} \\ \vec{r} = x \hat{x} + y \hat{y} + z \hat{z} \end{cases}$$

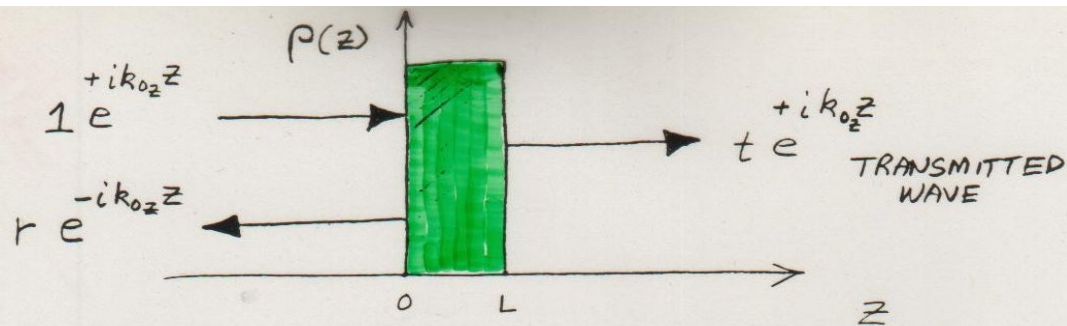
FOR \vec{k}_0 ALONG \hat{z} , FOR EXAMPLE,

$$\Psi \propto \cos(k_{0z} z) + i \sin(k_{0z} z)$$



$$\left(\frac{2\pi}{\lambda} z \right)$$

$|\Psi|^2 \propto$ PROBABILITY
OF THE
NEUTRON
BEING
THERE



$$Q = z k_{0z}$$

FROM THE WAVE EQUATION,
IT IS POSSIBLE TO FIND
A SOLUTION FOR THE
REFLECTION AMPLITUDE IN
INTEGRAL FORM
(SEE ARTICLE PAGES) :

$$r(Q) = \frac{4\pi}{iQ} \int_{-\infty}^{+\infty} \Psi(z) P(z) e^{+ik_{0z}z} dz$$

WHAT IS LOCALIZED AT z IN
THE SLD PROFILE $P(z)$ IN
"REAL" SPACE, IS DISTRIBUTED
OVER THE REFLECTION AMPLITUDE
 $r(Q)$ IN THE RELATED SCATTERING
OR "RECIPROCAL" SPACE

$\psi(z)$ INSIDE THE MEDIUM
IS GENERALLY UNKNOWN:

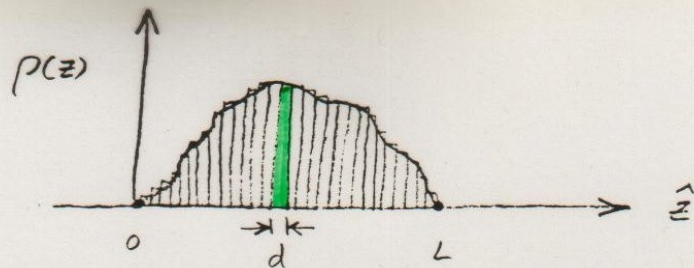
BORN APPROXIMATION REPLACES
 $\psi(z)$ WITH THE INCIDENT
WAVE FUNCTION e^{+ik_0z} BASED
ON THE ASSUMPTION THAT
 $\psi(z)$ IS NOT SIGNIFICANTLY
DISTORTED FROM THE FREE
SPACE FORM (WEAK
INTERACTION): THEN

$$r(Q) \approx \frac{4\pi}{iQ} \int_{-\infty}^{+\infty} p(z) e^{iQz} dz$$

FOURIER
TRANSFORM

FOR A REAL POTENTIAL $p(z)$

$$\text{Re } r(Q) \approx \frac{4\pi}{Q} \int_{-\infty}^{+\infty} p(z) \sin(Qz) dz$$



ARBITRARY POTENTIAL DIVIDED INTO
RECTANGULAR SLABS OF WIDTH
 d AND CONSTANT P

THEN

(BORN APPROX.)

$$\text{Re } r(Q) \approx \frac{4\pi}{Q} \int_0^L p(z) \sin(Qz) dz$$

BECOMES

$$\begin{aligned} \text{Re } r(Q_j) &\approx \frac{4\pi}{Q_j} \sum_{l=1}^N \int_{(l-1)d}^{ld} P_l \sin(Q_j z) dz \\ &= \frac{-4\pi}{Q_j^2} \sum_{l=1}^N P_l \left[\cos(Q_j z) \right]_{(l-1)d}^{ld} \end{aligned}$$

SET OF
Re r FOR
DIFFERENT
VALUES OF
 Q OR θ

$$\begin{cases} \text{Re } r_1 = C_{11} P_1 + C_{12} P_2 + \dots + C_{1N} P_N \\ \text{Re } r_2 = C_{21} P_1 + C_{22} P_2 + \dots + C_{2N} P_N \\ \vdots \\ \text{Re } r_N = C_{N1} P_1 + C_{N2} P_2 + \dots + C_{NN} P_N \end{cases}$$

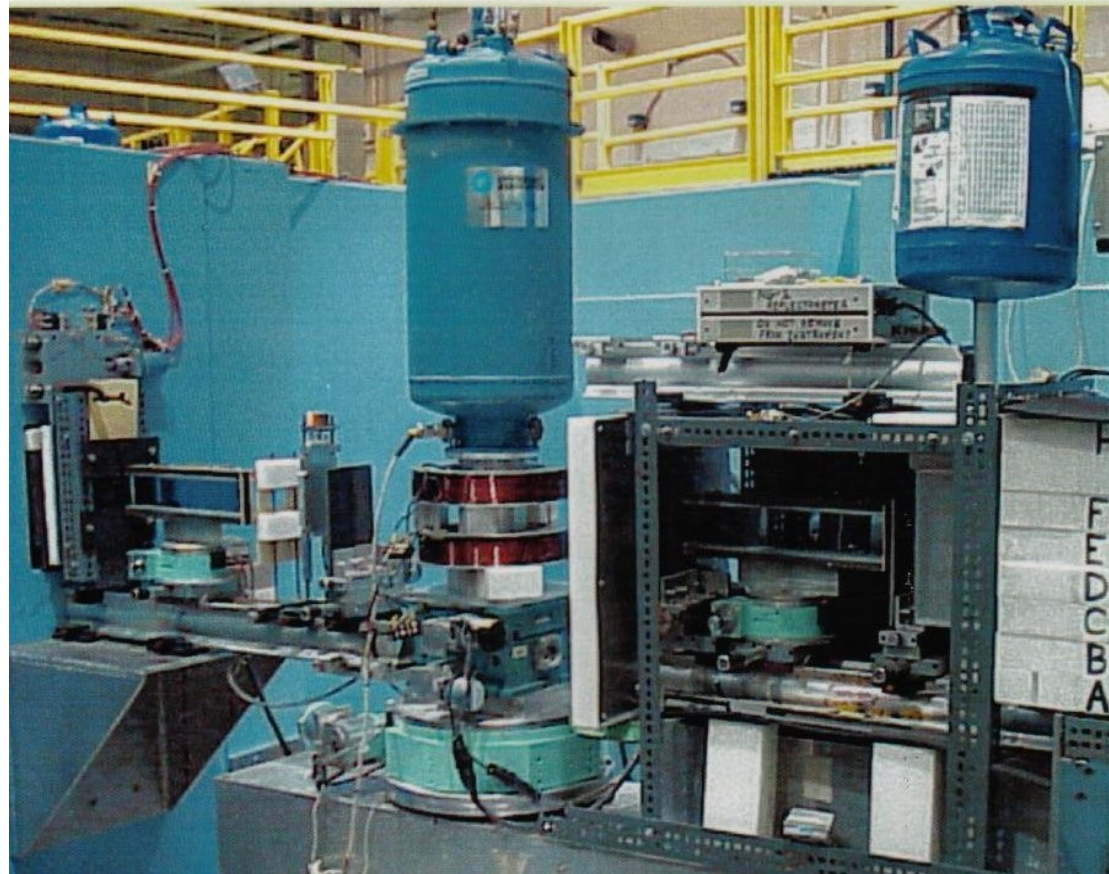
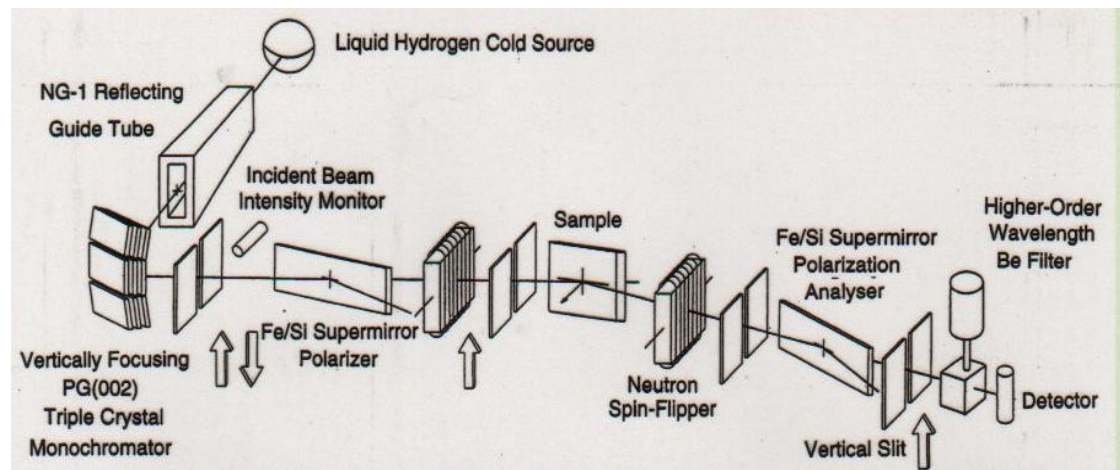
SOLVE SIMULTANEOUS EQUATIONS FOR P 's GIVEN $\text{Re } r$'s
e.g., SVD, EIGENVALUE PROBLEM FORMULATION, ...

$$\underbrace{\operatorname{Re} r_{Bn}(Q) \left[\frac{Q^2}{8\pi \sin\left(\frac{Qd}{2}\right)} \right]}_{\equiv I(Q)} = \sum_{j=1}^N \rho_j \sin\left[\frac{(2j-1)Qd}{2}\right]$$

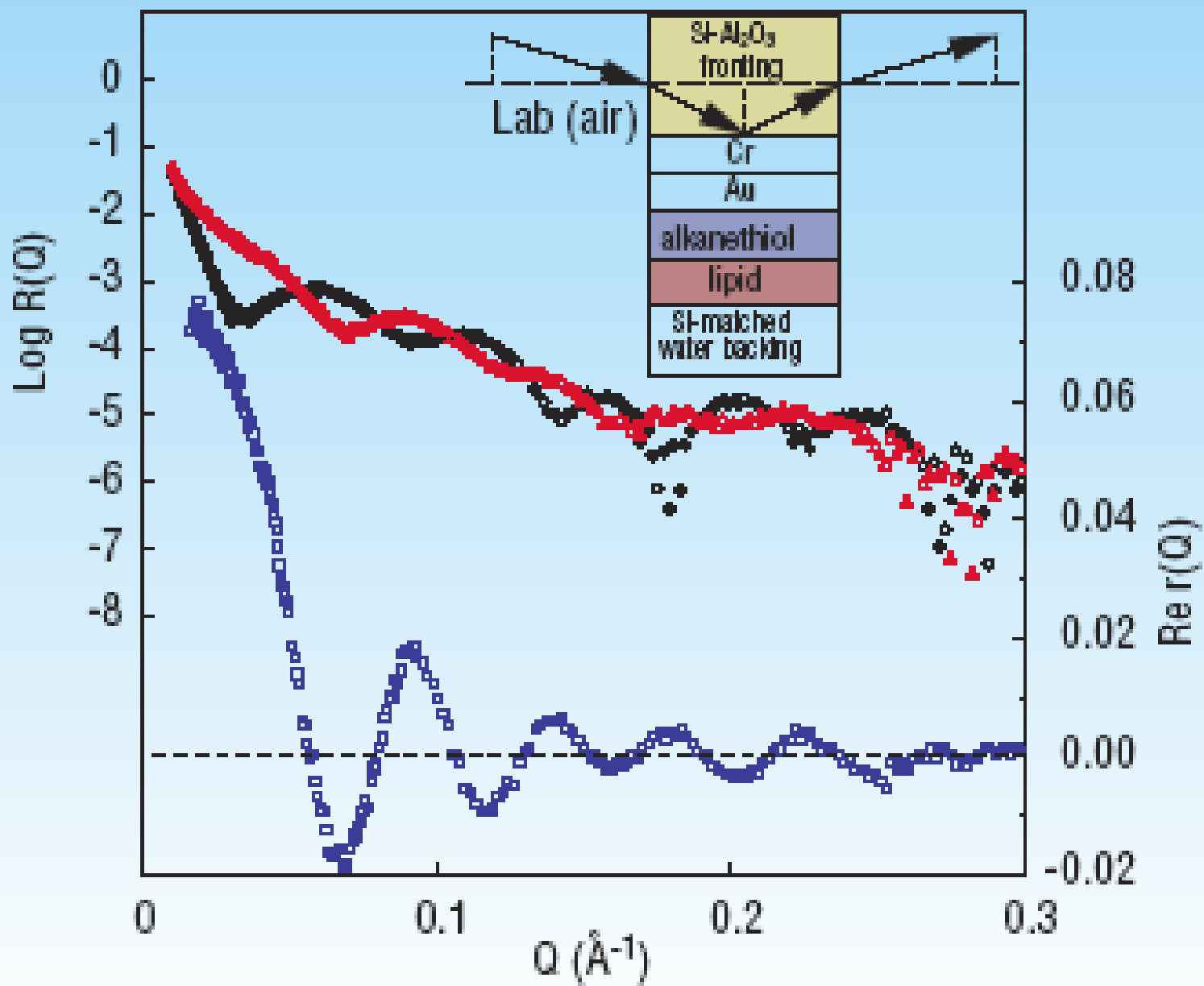
$$\int_0^{\pi} \sin m\theta \sin n\theta d\theta = \begin{cases} 0 & m, n \text{ INTEGERS, } m \neq n \\ \frac{\pi}{2} & m, n \text{ INTEGERS, } m = n \end{cases}$$

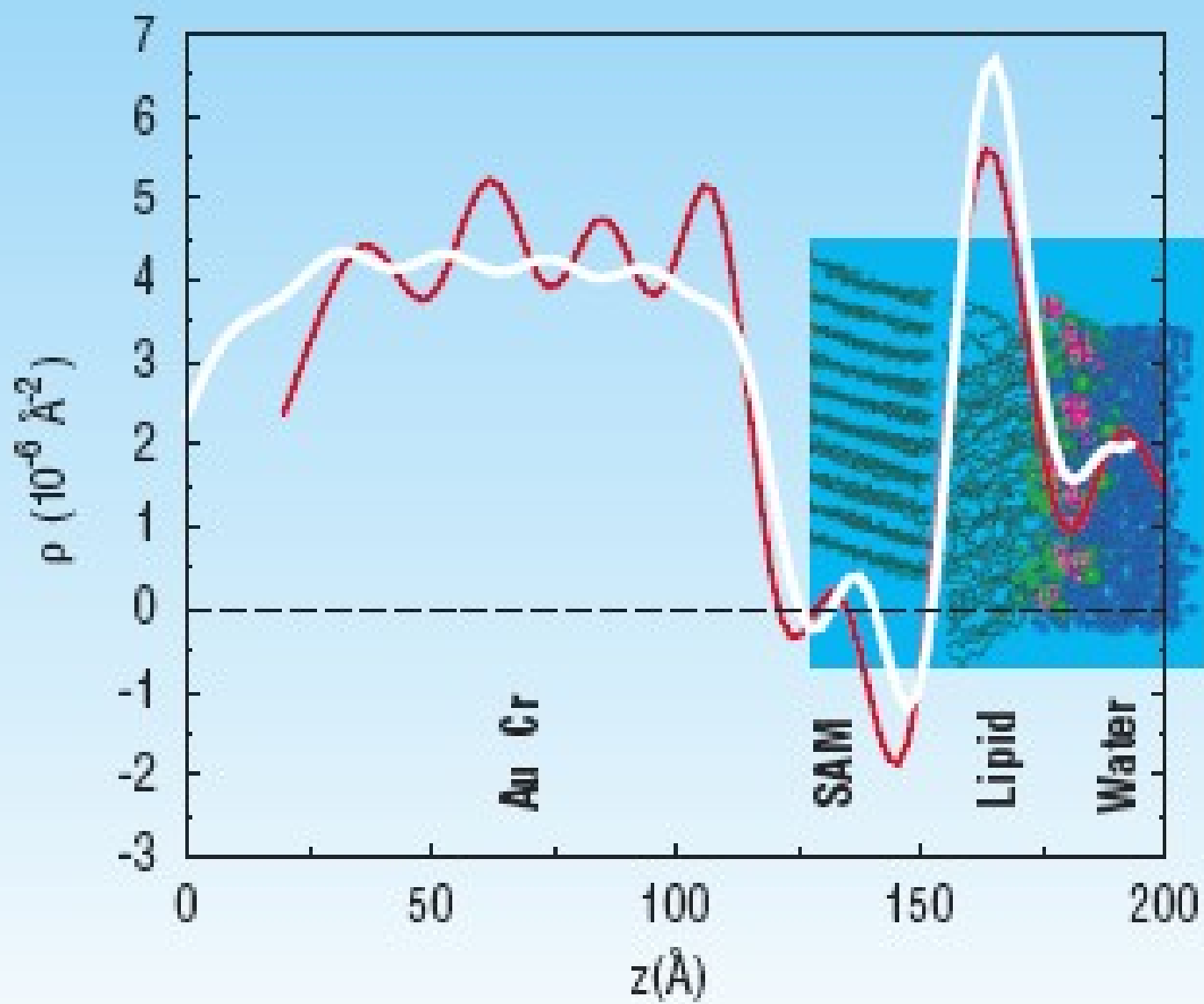
ORTHOGONALITY

$$\rho_j = \frac{d}{4\pi^2} \int_0^{\frac{\pi}{d}} Q^2 \operatorname{Re} r_{Bn}(Q) \frac{\sin\left[\frac{(2j-1)Qd}{2}\right]}{\sin\left(\frac{Qd}{2}\right)} dQ$$



Polarized neutron reflectometer/diffractometer at the NIST Center for Neutron Research.





Diblock copolymer lamellar nanostructures –
R.Jones, B.Berry, and K.Yager (NIST Polymer
Division) and S.Satija, J.Dura, B.Maranville et al.
(NCNR).

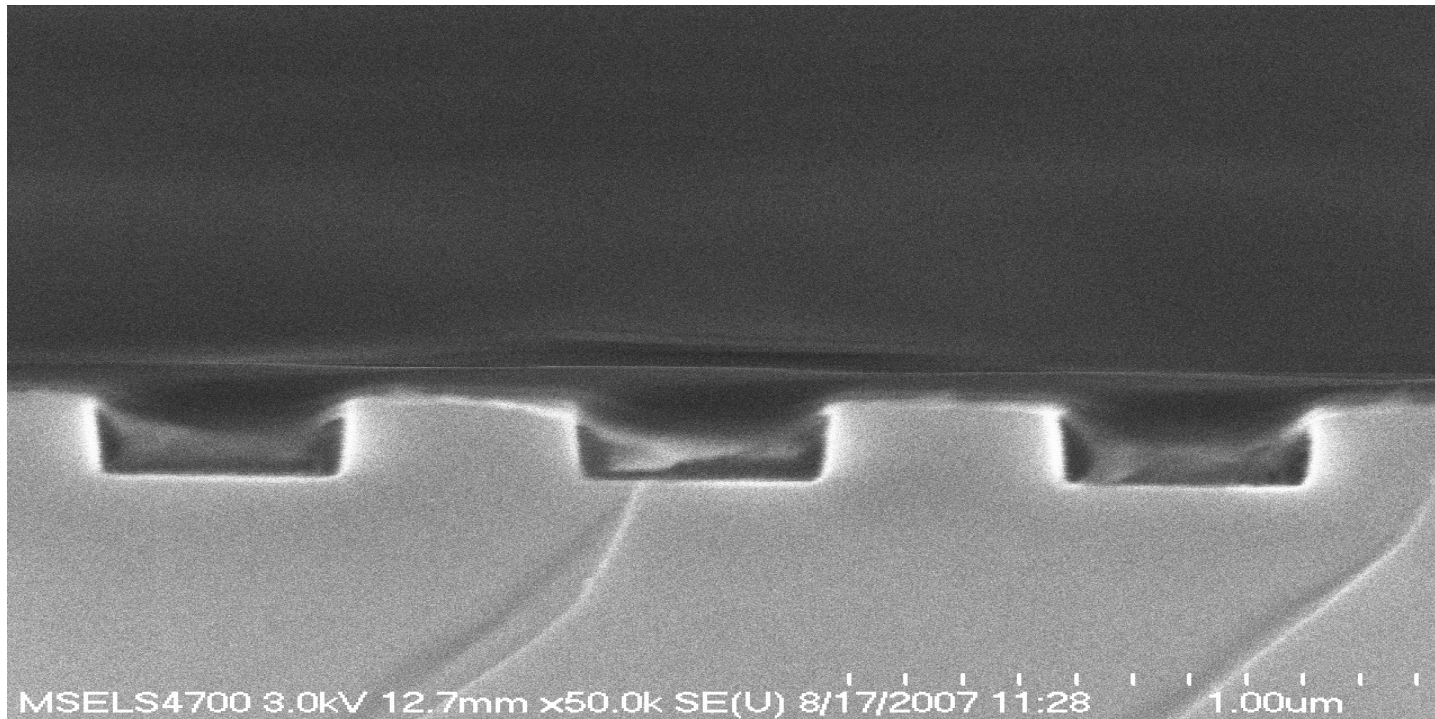
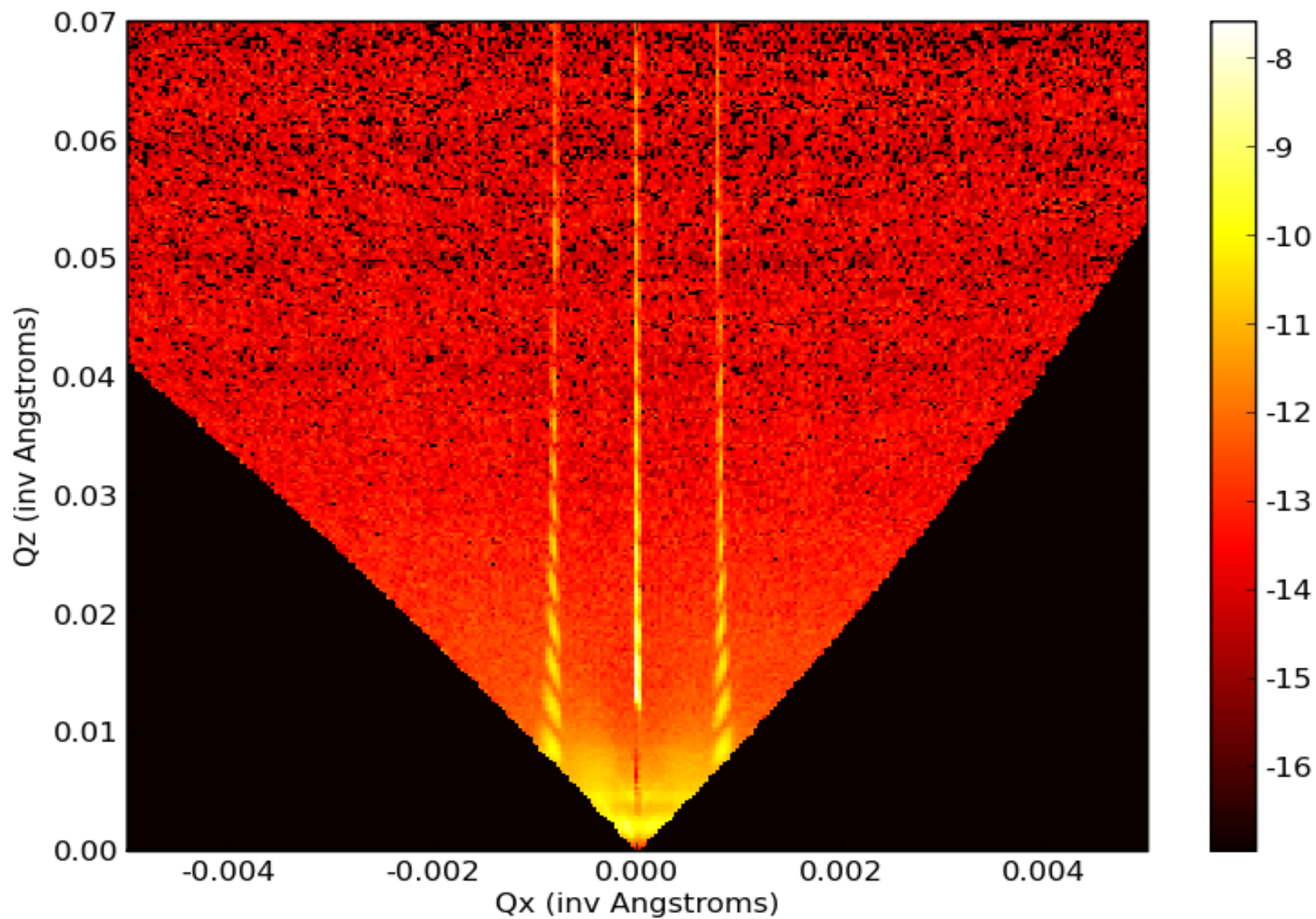


Fig 1. Side-view scanning-electron micrograph of laser-interferometry-produced silicon substrate with 400 nm channels, spaced by 400 nm for a total repeat distance of 800 nm.



Neutron diffraction from silicon with channels but without polymer.

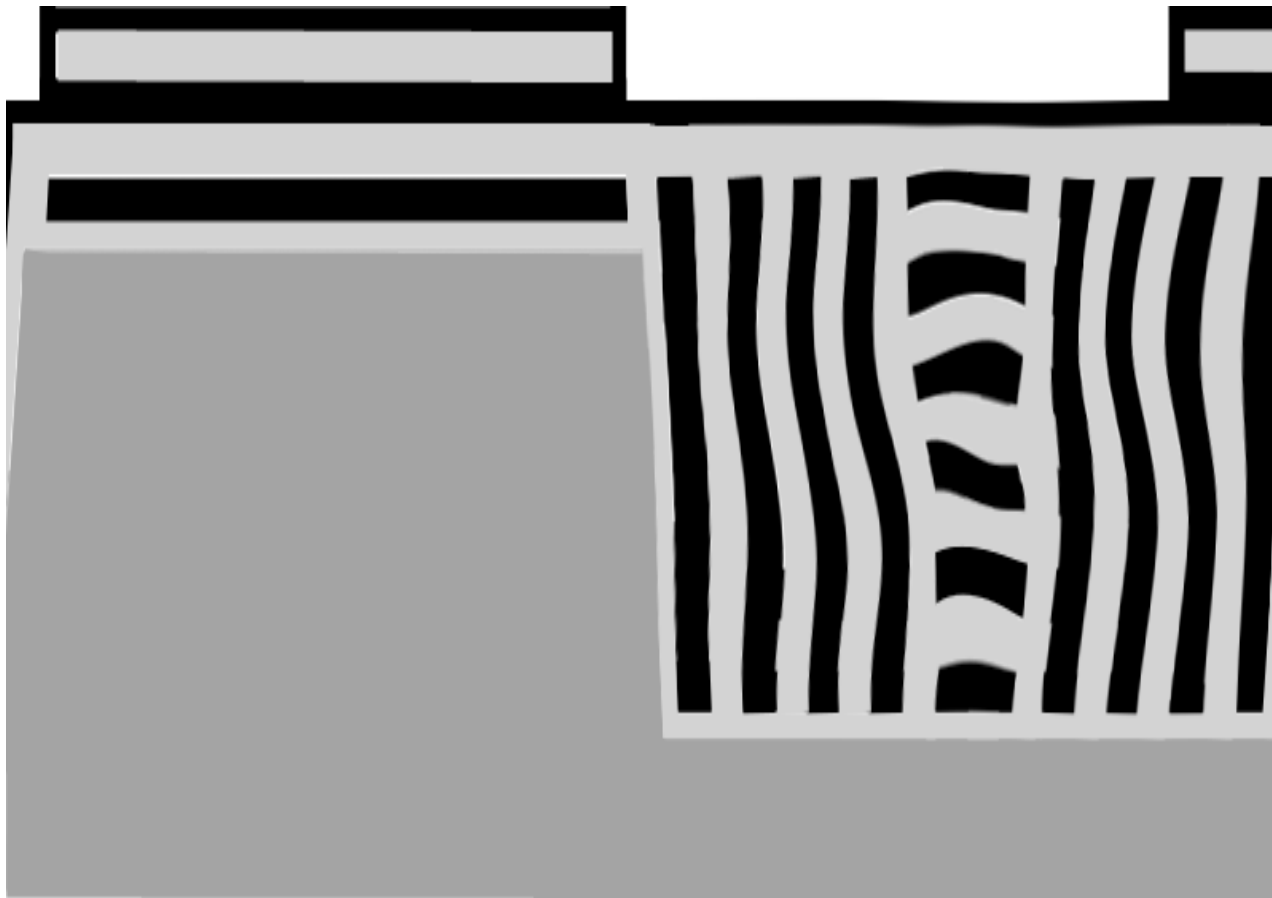
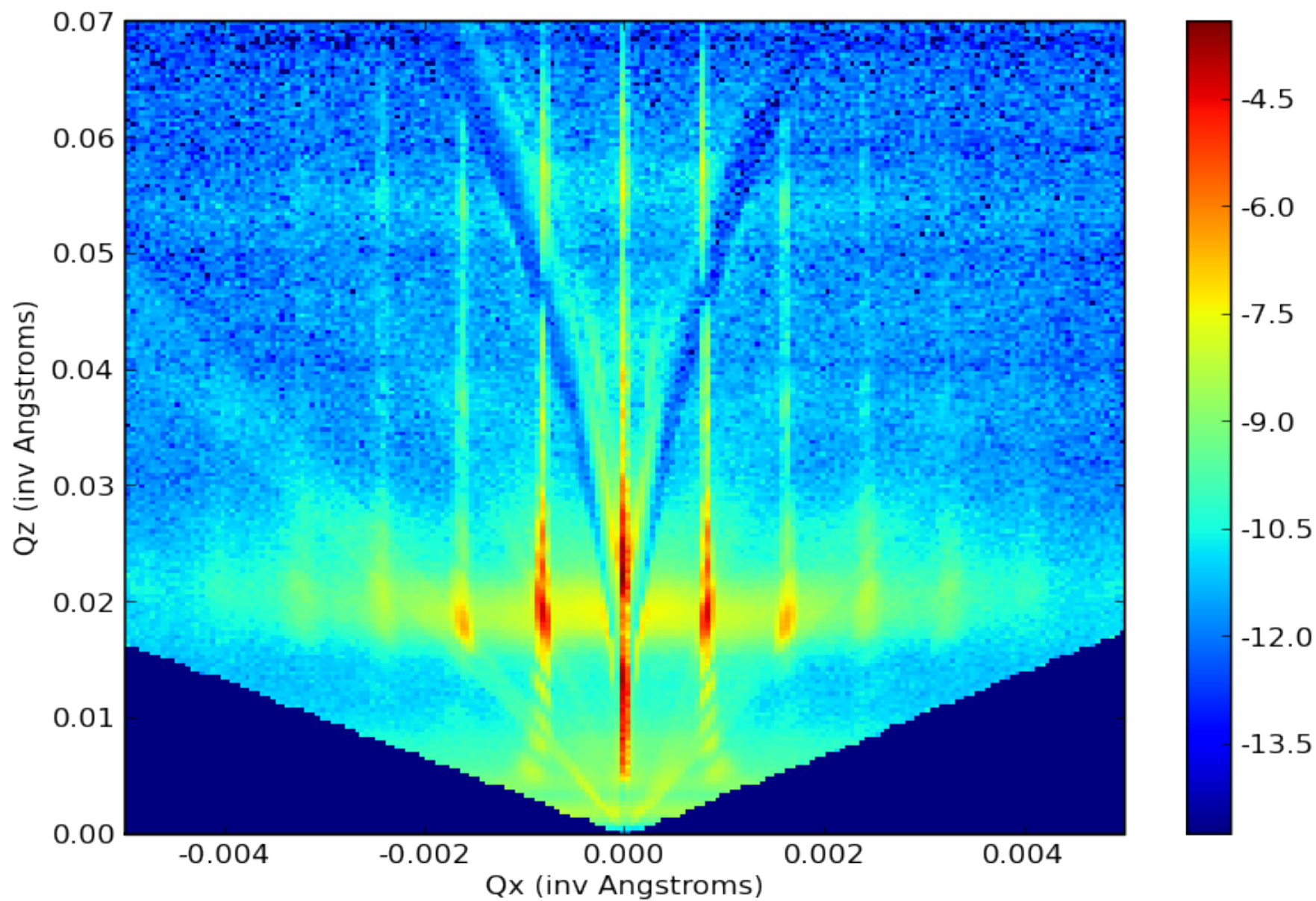
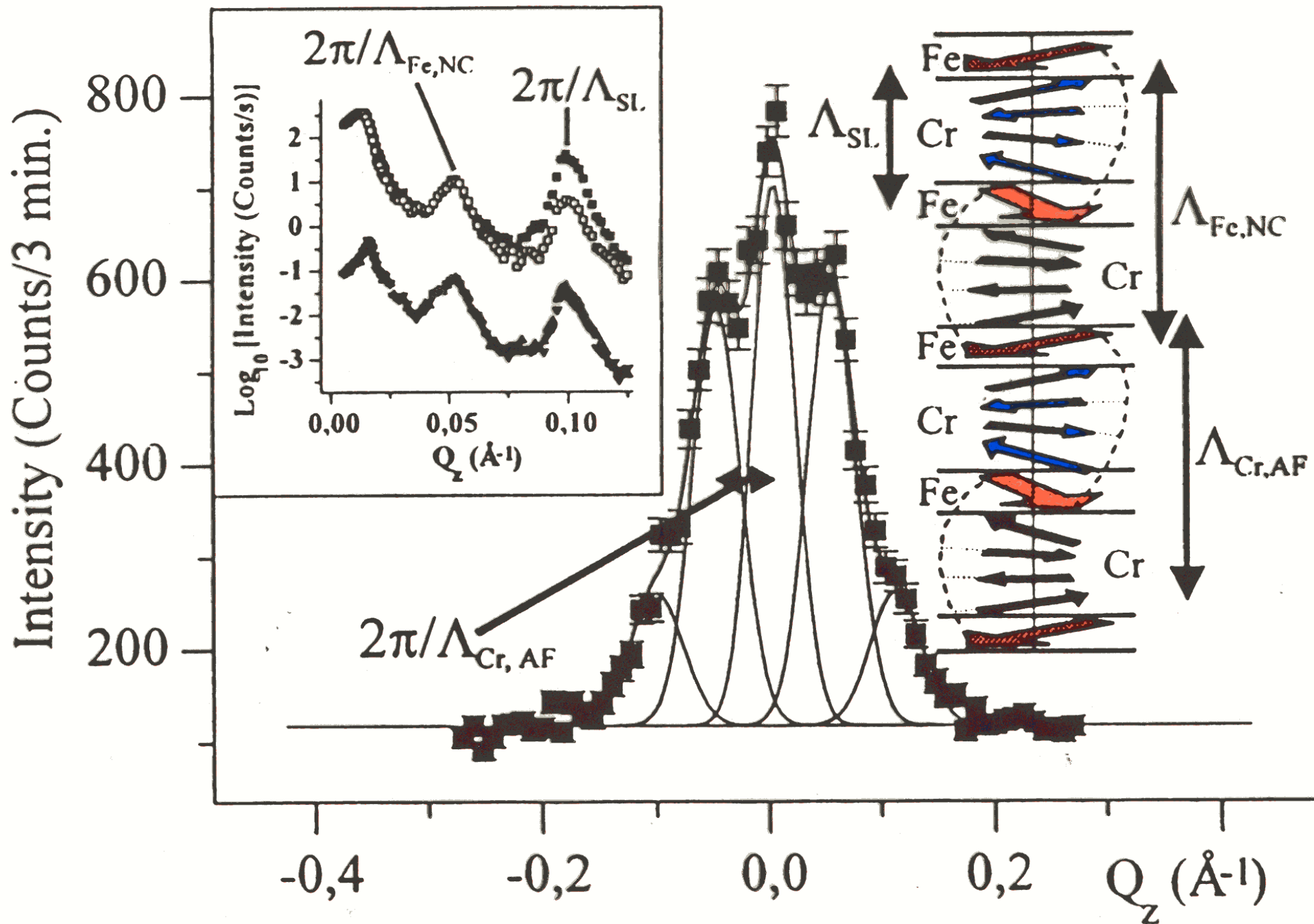


Fig 2. Diagram of expected orientation of lamellae, based on Silicon substrate with etched channels is displayed in gray, with corresponding to the two polymer components of the lamellae



Neutron diffraction from Si channels filled with ordered diblock copolymer.



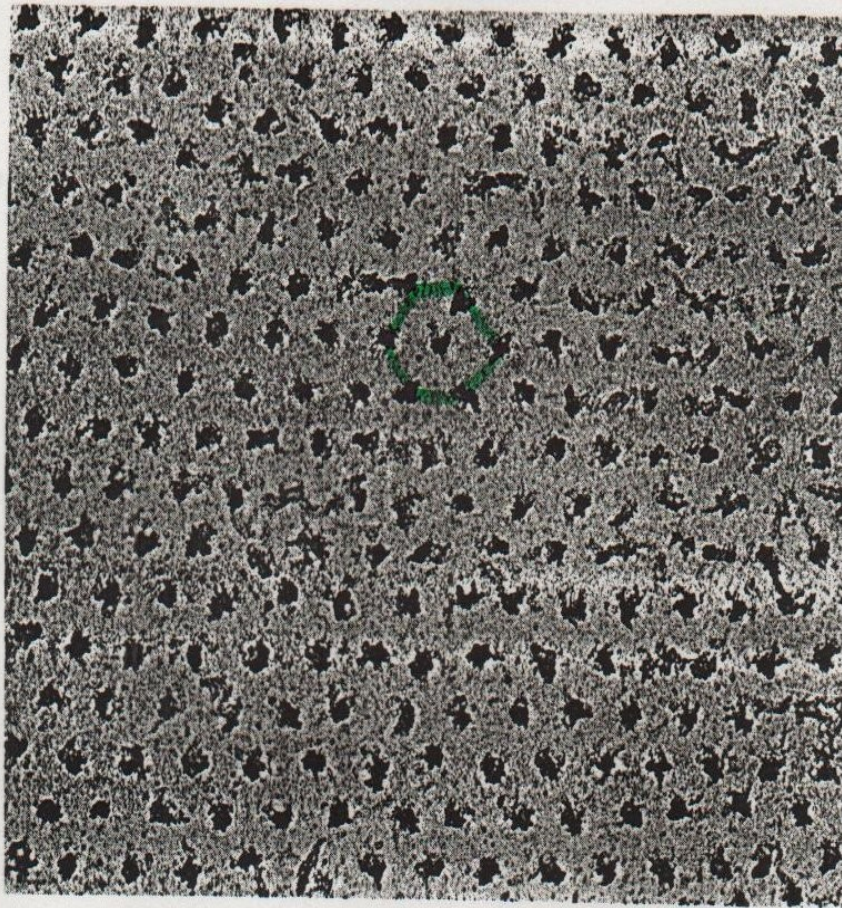
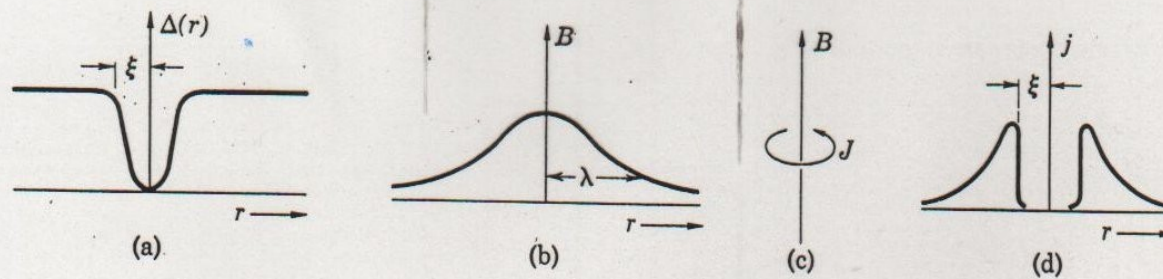
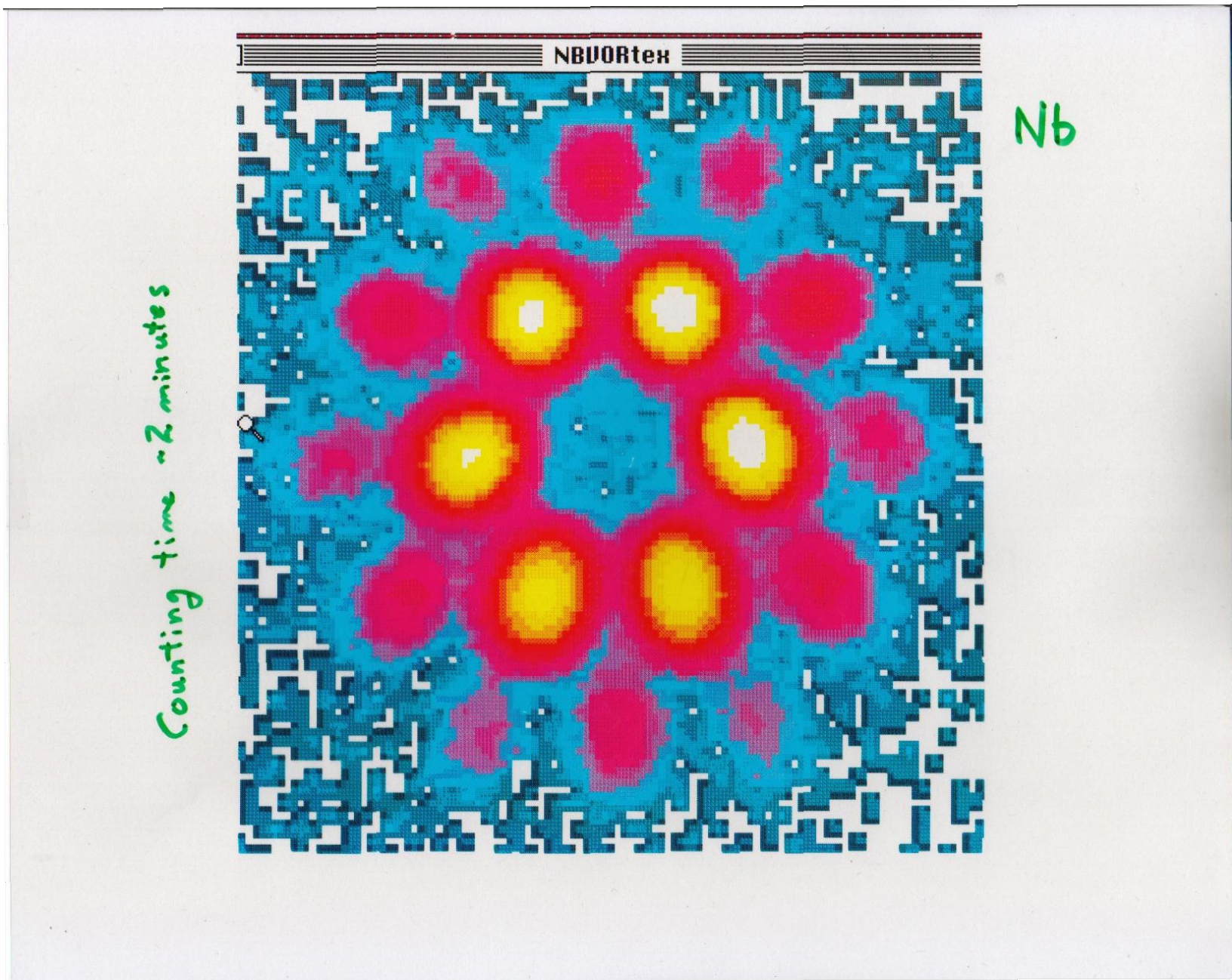
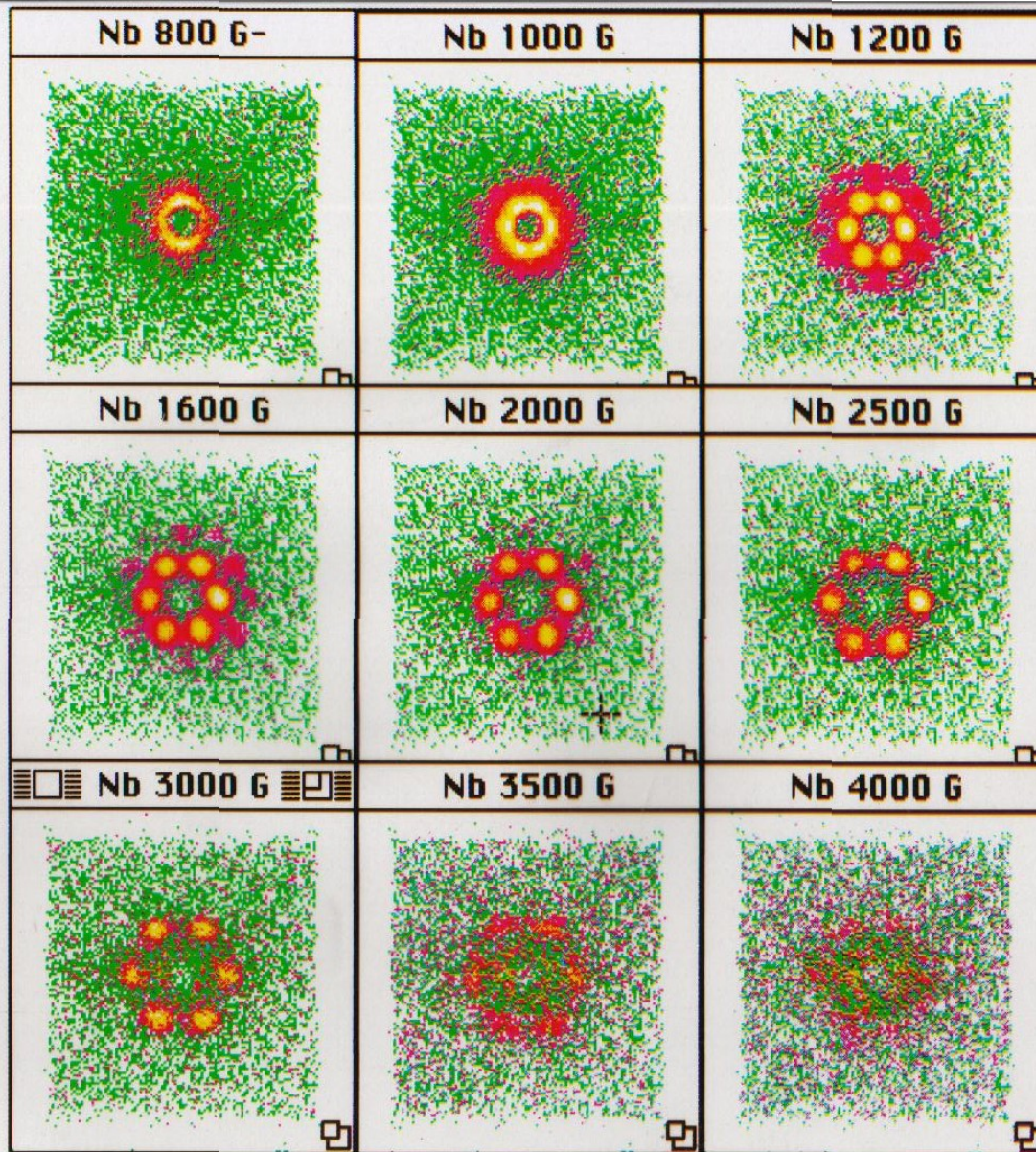


Figure 37 Triangular lattice of flux lines through top surface of a superconducting cylinder. The points of exit of the flux lines are decorated with fine ferromagnetic particles. The electron microscope image is at a magnification of 8300..(Courtesy of U. Essmann and H. Träuble.)





SANS diffraction pattern of vortex lattice in superconducting Nb – J.Lynn et al..



$T \approx 4.4 \text{ K}$

Vortex Lattice Dynamics in Niobium

J.W. Lynn, et al, Phys. Rev. Lett. 72, 3413 (1994)